

2015-05-01

# Devonian Shale Petrophysical Study and Modelling

Zhang, Xianfeng

---

Zhang, X. (2015). Devonian Shale Petrophysical Study and Modelling (Master's thesis, University of Calgary, Calgary, Canada). Retrieved from <https://prism.ucalgary.ca>. doi:10.11575/PRISM/25696  
<http://hdl.handle.net/11023/2221>

*Downloaded from PRISM Repository, University of Calgary*

UNIVERSITY OF CALGARY

Devonian Shale Petrophysical Study and Modelling

by

Xianfeng Zhang

A THESIS

SUBMITTED TO THE FACULTY OF GRADUATE STUDIES  
IN PARTIAL FULFILMENT OF THE REQUIREMENTS FOR THE  
DEGREE OF MASTER OF SCIENCE

GRADUATE PROGRAM IN GEOLOGY AND GEOPHYSICS

CALGARY, ALBERTA

APRIL, 2015

© Xianfeng Zhang 2015

## **Abstract**

A major issue petroleum companies have with unconventional resource plays, is identifying prospective areas early in exploration stage. Early land captures of contiguous blocks at reasonable entry, exploration and appraisal costs are critical to the economic success of the program. The Duvernay shale play in Western Canada is an excellent example of an emerging play. During exploration efforts, the Kaybob area was identified as highly prospective.

This study takes advantage of this emerging play to illustrate the use of logs, calibrated with core to identify and characterize prospective zones in the Duvernay Shale. Well log facies and petrophysical parameters based on 3-D static models were used to determine the production potential within the Kaybob area and the associated uncertainty.

The model result and the first three months normalized production comparison show positive trends. The result also indicates that there are multiple factors that contribute to a good producing well.

## **Acknowledgements**

First, I want to thank Dr. Laurence R. Lines for his supervision, and my previous supervisor Dr. Robert R. Stewart for accepting me as a graduate student. At the same time, I appreciate Dr. Roberto Aguilera and Dr. John C. Bancroft as the defense committee members for giving me many good suggestions and recommendations for improving my thesis. I would also like to thank Catherine Hubbell and Faye Nicholson for providing all the detailed information requires to finish.

Secondly, I would like to thank Nexen for supporting my thesis work, giving me access to all the data in the study area, and letting me to use all the software and tools.

Thirdly, thanks to CoreLab for allowing me use their “CoreClientWeb” data. The data set gave me the chance to have enough Duvernay core data (4 out 8 used cored wells) to calibrate logs, for building a petrophysical model. For confidential purposes, none of the wells’ names were mentioned, and only part of the depth can be seen.

I would like to say thanks to my colleagues from Unconventional Exploration and Petrophysics department at Nexen. I will always appreciate and remember your help, which added extra burden along with your busy daily workloads.

Special thanks to Dr. David Campagna, without your guidance, encouragement, and support, I could not finish this thesis.

Last but not least, I want to say thanks to my wife and two lovely kids, and I will spend more time with you, since my thesis work is accomplished.

## Table of Contents

Abstract.....	ii
Acknowledgements .....	iii
Table of Contents.....	iv
List of Figures.....	vi
List of Table.....	ix
List of Symbols, Abbreviations, Nomenclatures.....	x
<b>Chapter 1: Introduction .....</b>	<b>1</b>
1.1 Background.....	1
1.2 Stratigraphic overview .....	2
1.3 Devonian shale regional structural setting.....	4
1.4 Regional Depositional Model.....	4
1.5 Duvernay activity .....	7
1.6 Target interval.....	7
1.7 Study Objective and methodology .....	8
<b>Chapter 2: Petrophysical 1D model calibrated with core data.....</b>	<b>10</b>
2.1 Core/log data quality control .....	10
2.2 Log data package .....	12
2.3 Petrophysical properties .....	12
2.4 The petrophysical model to core comparison.....	27
<b>Chapter 3: Petrophysical facies building.....</b>	<b>44</b>
3.1 MRGC facies .....	44
3.2 Model building.....	45

<b>Chapter 4: 3-D model building</b> .....	<b>50</b>
4.1 study Area .....	50
4.2 Petrel 3-D output.....	51
<b>Chapter 5: Comparison of the model result to production data</b> .....	<b>59</b>
5.1 Duvernay Kaybob area production distribution.....	59
5.2 Facies and production relationship.....	60
5.3 High grading area of greater than 10 meters in facies 2.....	69
<b>Chapter 6: Experimental results and discussion</b> .....	<b>71</b>
<b>Conclusions</b> .....	<b>72</b>
<b>Bibliography</b> .....	<b>73</b>

## List of Figures

Figure 1.1.1 Index map of the Duvernay Formation.....	1
Figure 1.2.1 Duvernay stratigraphic chart.....	3
Figure.1.3.1 Devonian shales regional structural setting .....	4
Figure 1.4.1 Paleogeographic maps .....	5
Figure 1.4.2 Duvernay deposition and rock lithology.....	6
Figure 1.6.1 Study Area .....	8
Figure 2.1.1 Core points shift based on the core GR and log GR matching....	10
Figure 2.1.2 Core depth shifted result .....	11
Figure 2.3.1 Clay vs. DIFFND cross plot.....	14
Figure 2.3.2 Clay vs. GR cross plot.....	15
Figure 2.3.3 Core Grain Density vs. Log Derived Grain Density.....	17
Figure 2.3.4 Core porosity vs. Log derived porosity.....	18
Figure 2.3.5 well G logs layout .....	19
Figure 2.3.6 well G Core porosity vs. Log derived porosity.....	20
Figure 2.3.7 Pickett plot (m=1.7, n=2.4).....	23
Figure 2.3.8 Pickett plot with different slope angle ( different m).....	24
Figure 2.3.9 Pickett plot with different Archie saturation exponent (n) .....	24
Figure 2.3.10 Schematic guide of $\Delta\log R$ response .....	25
Figure 2.3.11 Delta Log R method applied to Density-Resistivity logs.....	26
Figure 2.4.1 well A final layout.....	31
Figure 2.4.2 well B final layout.....	32
Figure 2.4.3 well C final layout.....	33

Figure 2.4.4 well D final layout.....	34
Figure 2.4.5 well E final layout.....	36
Figure 2.4.6 well F final layout.....	37
Figure 2.4.7 well G final layout.....	38
Figure 2.4.8 well H final layout.....	39
Figure 2.5.1 Preliminary porosity average plot.....	41
Figure 2.5.2 Well I plot.....	42
Figure 2.5.3 Well J plot.....	43
Figure 3.1.1 Three main petrophysical import distributions histogram.....	45
Figure 3.2.1 MRGC Model Parameters.....	46
Figure 3.2.2 MRGC_7_CLUST three inputs crossplot.....	48
Figure 3.2.3 Facies detail distribution.....	49
Figure 4.1.1 Duvernay working region and well location map.....	50
Figure 4.1.2 Duvernay formation in Petrel 3-D.....	51
Figure 4.2.1 BVH net plot.....	52
Figure 4.2.2 Average Clay plot.....	53
Figure 4.2.3 Low porosity facies 6 & 1 average thickness in Duvernay.....	54
Figure 4.2.4 Carbonate facies average thickness in Duvernay.....	55
Figure 4.2.5 Facise 2 average thickness in Duvernay.....	56
Figure 4.2.6 Facise 3 average thickness in Duvernay.....	57
Figure 5.1.1 Duvernay Kaybob area liquid production rate.....	59
Figure 5.1.2 Duvernay Kaybob area liquid production rate (without water).....	60
Figure 5.2.1 Duvernay Kaybob well production vs. facies thickness.....	62

Figure 5.2.2 facies 2 thickness vs. production.....	66
Figure 5.2.3 facies 2 thickness (< 10m) vs. production.....	67
Figure 5.2.4 facies 2 thickness (> 10m) vs. production .....	68
Figure 5.3.1 Facies 2 high grading area with 10 meters cut off.....	70

## List of Table

Table 2.1.1 Core wells depth correction.....	11
Table 3.2.1 MRGC_7_CLUST mean values for different facies.....	46
Table 5.2.1 DVRN Kaybob area first three month normalized hydrocarbon day rate...	63

## List of Symbols, Abbreviations, Nomenclature

a	Archie cementation constant
BVH	Bulk volume hydrocarbon, v/v
CC	Correlation coefficient
DIFFND	The difference between neutron limestone porosity and density limestone porosity, v/v
DPHI	Density limestone porosity, v/v
GR	Gamma ray log, API
m	Archie cementation exponent
n	Archie saturation exponent
NMR	Nuclear magnetic resonance log
NPHI	Neutron limestone porosity, v/v
Phie	Effective porosity, v/v
Phit	Total porosity, v/v
RHOB	Bulk density, g/cc
RHOF	Fluid density, g/cc
RHOG	Grain density, g/cc
RT	True formation resistivity, ohm*m
Rw	Connate-brine resistivity, ohm*m
Swt	Total water saturation, v/v
TOC	Total organic carbon, w%
TOC_ΔLogR	Passey method calculated total organic carbon, w%
TOC_GR	Gamma ray log calculated total organic carbon, w%
V <sub>clay</sub>	Log calculated clay volume, v/v
V <sub>clay_GR</sub>	Clay volume, calculated from gamma ray log, v/v
V <sub>clay_ND</sub>	Clay volume, calculated from neutron density log, v/v
Vol_calcite	Carbonate volume, v/v
Vol_illite	Clay volume, v/v
Vol_quartz	Sandstone volume, v/v
Vro	Vitrinite reflectance
Φ <sub>D</sub>	Density Porosity, v/v
Φ <sub>T</sub>	Total porosity, v/v

# Chapter 1: Introduction

## 1.1 Background

One major issue in unconventional resources is identifying prospective areas early in the exploration stage. The Devonian Duvernay shale play in Western Canada is an excellent example of an emerging play, and the Kaybob area (Figure 1.1.1) was identified as highly prospective.

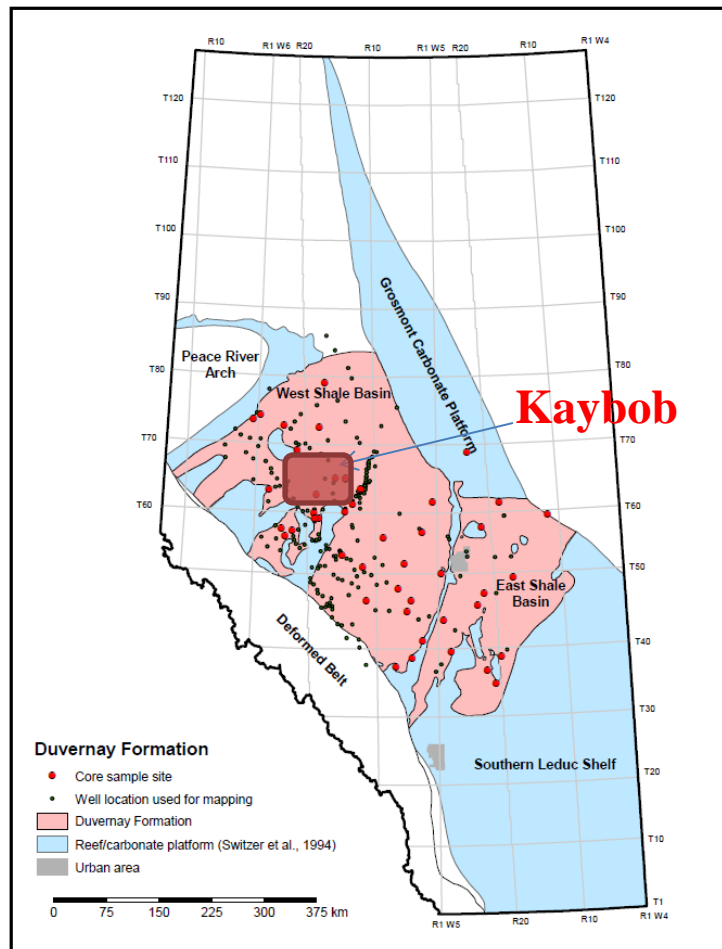


Figure 1.1.1 Index map of the Duvernay Formation (modified from Rokosh et al., 2012)

The Duvernay Formation (Duvernay) is an Upper Devonian source rock in central Alberta, and it is known to have sourced the Leduc and Swan Hills oil and gas reservoirs (Rokosh et al., 2012).

## 1.2 Stratigraphic overview

The Duvernay formation is located in the central plains area of the Western Canadian Sedimentary Basin, and is equivalent to the Muskwa, Canol and Hare Indian formations of the late Devonian, Frasnian condensed section as shown in Figure 1.2.1. Duvernay is deposited disconformably above the carbonates and marls of the Majeau Lake, Cooking Lake and Beaverhill Lake group during a transgression, and it is overlain by the highstand to progradational deposition of the more clastic rich, basin filling Ireton and Fort Simpson shales.

REGIONAL PLAY FAIRWAY MAPPING

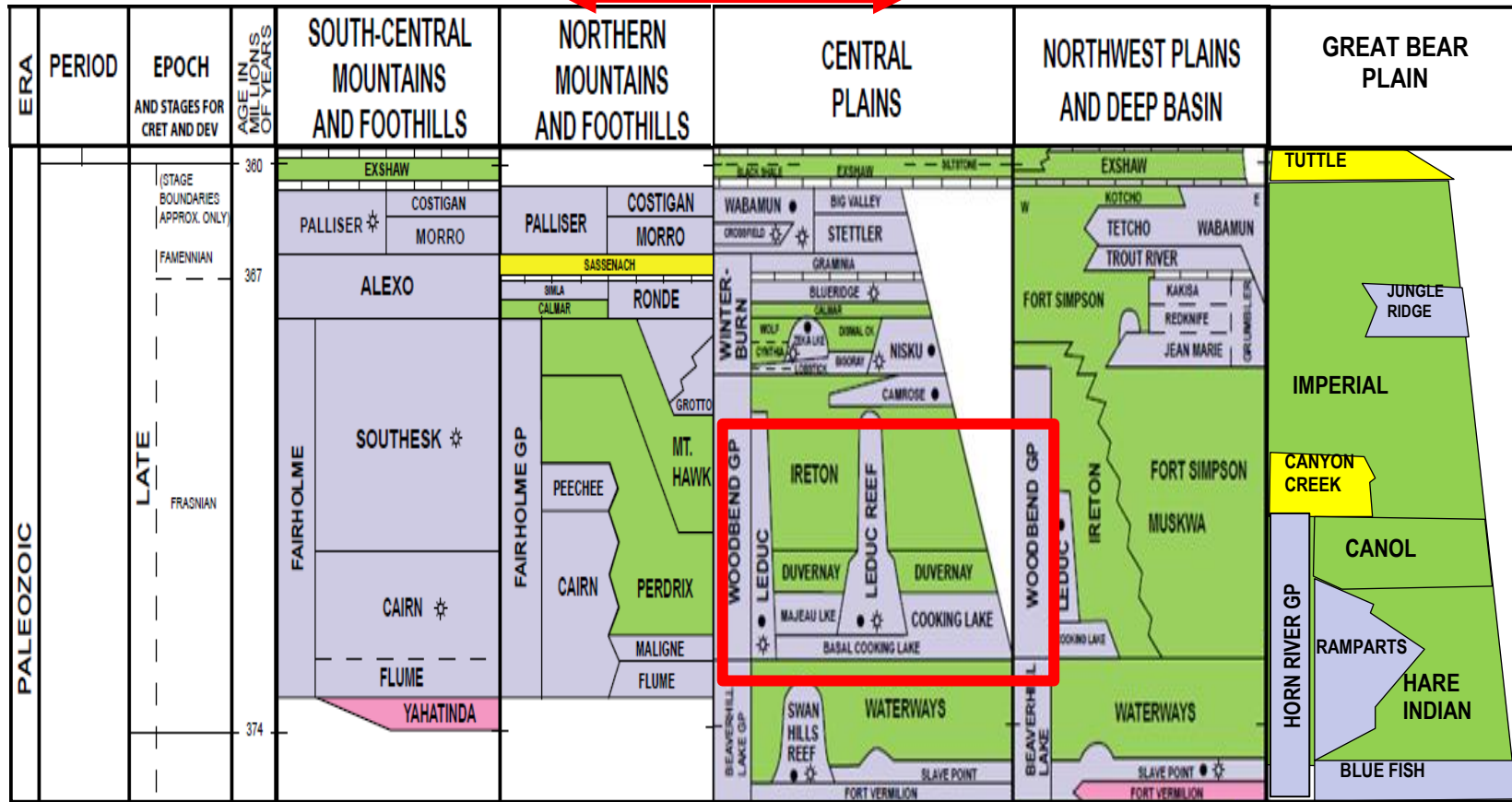


Figure 1.2.1 Duvernay stratigraphic chart

### 1.3 Devonian shale regional structural setting

As Figure 1.3.1 (Misko, 2014) shows, the Duvernay age (green shaded area) equivalent facies is impacted by cratonic uplift and topographic high (Peace River Arch), grabens, normal / reverse faulting and shear zone segments. Syndepositional structural disruption, related to tectonically active basement lineaments, impacts character and thickness along with reef and carbonate platform development near the basin margins.

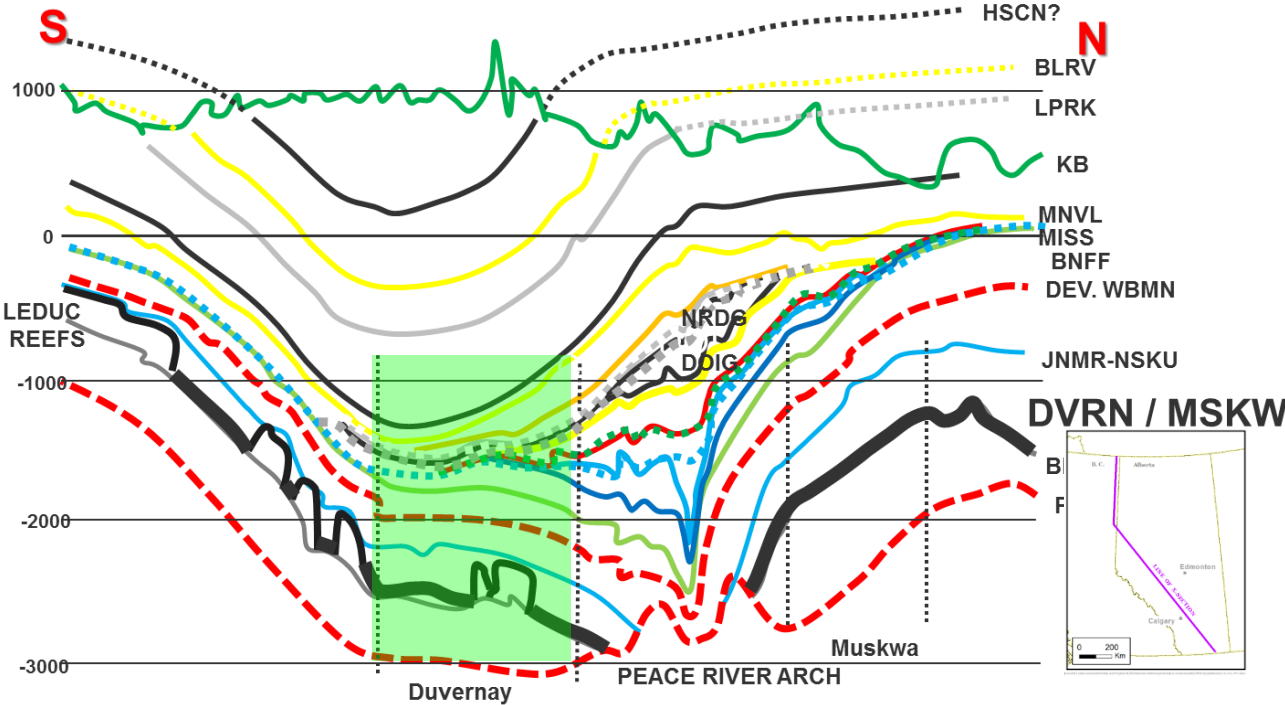


Figure.1.3.1 Devonian shales regional structural setting (After Ron Misko, Nexen, 2014)

### 1.4 Regional Depositional Model

Devonian Shales sediment source, transport and ocean currents contributed to high quality shale depositional centers. Ocean current direction varies depending on the location of the equator (white line in Figure 1.4.1). The mineral source of the Duvernay is a combination of siliceous, organic rich shale sourced by upwelling currents from the

west, and Aeolian sedimentation sourced from the east. The distribution of sediment was determined by the direction of ocean currents and wind direction, and the Aeolian sedimentation sourced from the east.



Figure 1.4.1 Paleogeographic maps adapted from Blakey, 1996



The Duvernay formation is up to 110 m thick (CSUR Presentation), and increases in maturity from east to west. The thickness, high source rock quality and desired maturity give the Duvernay the “potential to form the foundation of unconventional gas development in Alberta in the future” (Dawson, 2012).

### 1.5 Duvernay activity

The Duvernay shale is considered as “The New Millennium Gold Rush” – BMO Capital Markets (Low, 2012)

Based on Stastny’s (2013) study, the economics of the Duvernay stands on condensate-rich production. EnCana was spending \$600 million (along with PetroChina's Canadian subsidiary) in the play with 13 wells drilled on a rig release basis. The best well has produced a widely publicized 1,400 bbls/d of condensate and  $4 \times 10^6$  ft<sup>3</sup>/d of natural gas for the first 30 days.

Celtic/Yoho have tested three Duvernay horizontal wells at over  $3 \times 10^6$  ft<sup>3</sup>/d natural gas plus 75 barrels natural gas liquid near the Kaybob region of west central Alberta, based on CSUR 2011 Seminar. Regarding land sales, “in 2011 added over \$1 Billion in bonus bids to government as companies targeted Duvernay land rights in western Alberta” (Dawson, 2012).

There are many energy companies involved in Duvernay Kaybob area exploration and development. Those activities provided numerous modern logs, which are critical for this study.

### 1.6 Target interval

Based on the industry activities and various resources, the focused study area is limited to the Duvernay Kaybob area, as Figure 1.6.1. Higher quality undiluted shale

forms the target interval within the Upper Duvernay. Lateral extents are formed by the quality reduction of the condensed section to the south and east due to the carbonate platform, and to the north and west due to reefs and the impact of the Peace River Arch.



Figure 1.6.1 Study Area

## 1.7 Study Objective and methodology

This study takes advantage of this emerging play, to understand how to use logs to characterize the Kaybob area, and how to use core-calibrated petrophysical log analysis to identify prospective areas and zones.

Tasks and tools to be used in each solution included:

1. Software - GeoLog: for all the petrophysical works, to derive:
  - i.  $\text{Phit/Swt/Vclay/TOC}$
  - ii. Discussion of vertical heterogeneity
  - iii. Electron facies for Duvernay

- Petrel: modelling software, for geological model building
- SpotFire: data management software, for data comparison and screening

## 2. Data collection:

Core - GRI, XRD, RockEval, Thin section, from public data package and four wells from CoreLab consortium website - CoreClientWeb.

Log data - from Nexen owned LAS, which come from various resources. The total wells could be over one thousand, but I will only use a maximum of 200 wells to build a relative local model.

Formation tops, mostly from Nexen internal geologists' picking.

## Chapter 2: Petrophysical 1D model calibrated with core data

### 2.1 Core/log data quality control

The core-log relationship is the building block for petrophysical methodology. To shift the core interval to log depth is the first step, building the correlation between core and logs follows.

The standard core depth shift is based on the core gamma ray (black curve in the first track, Figure 2.1.1) moving up and down (moved up 7.5 meters in this case) to match the log gamma ray (Green curve); then the core points will be considered at the correct position after the shift accordingly; however, blue bulk density points, refer to red circles, are slightly misaligned with to the density log characters (RHOB, red curve in the same track). After the 0.5 meters (total 8 meters) further shift up, the log character seems to match the well in Figure 2.1.2.

In summary, the core to log depth matching procedure starts with the gamma ray guided data points depth shifting; then, is followed by a slight bulk density characters guided depth adjustment.

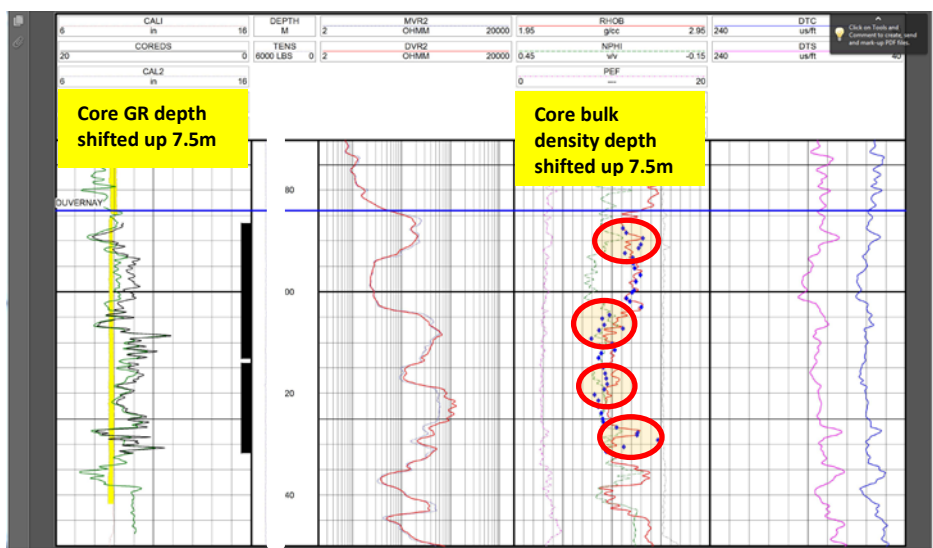


Figure 2.1.1 Core points shift based on the core GR and log GR matching

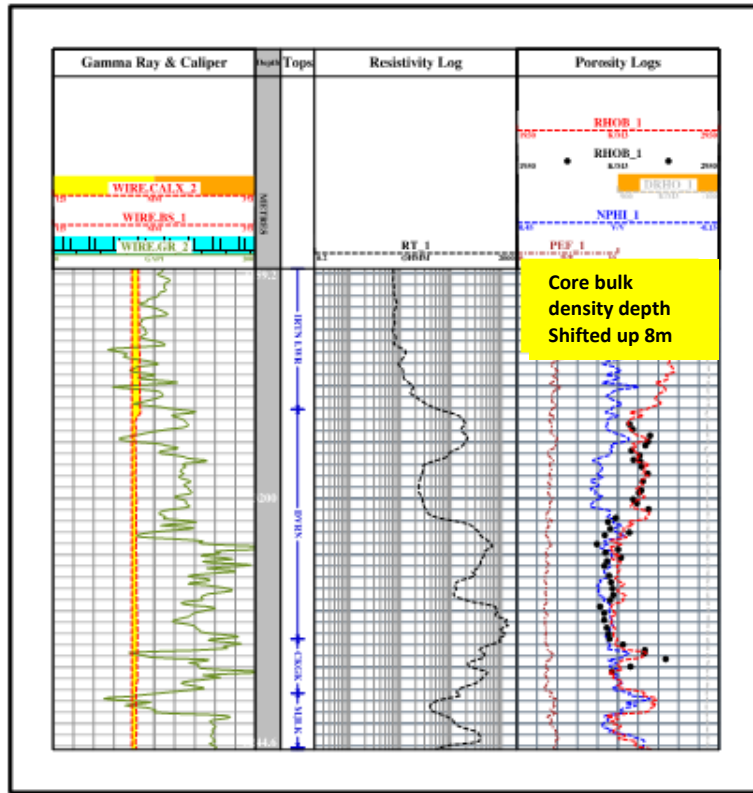


Figure 2.1.2 Core depth shifted result

Similar to the example well, other core wells have been depth shifted shown in the table 2.1.1

Table 2.1.1 Core wells depth correction

Well	Shifted Depth (m)
A	5
B	-8
C	3.5
D	1.7
E	0
F	4
G	5.3
H	4

## 2.2 Log data package

Due to the limitation of data availability for exploration purposes, the log data is only collected from public data resources, like IHS. Given this, the unconventional reservoirs full logs package, including the imaging log data, mineral log data, and NMR log data, usually are not available.

For the unconventional study, pore space, hydrocarbon volume, TOC richness, and formation fracability and potential frac barriers are the key characters; therefore, GR, Neutron/Density, and Resistivity are selected to meet the minimum requirement.

## 2.3 Petrophysical properties

Typical unconventional reservoirs have relative high GR reading, low Density log, high Neutron, and high Resistivity log reading, due to the organic matter log response; therefore, the unconventional petrophysical interpretation is very different from conventional.

### 2.3.1 Clay volume

With the uranium richness, a simple GR method cannot be used for clay volume calculation directly in a TOC (total organic carbon) rich zone; Neutron Density separation will give a close answer for clay volume.

As Figure 2.3.1 shows, clay volume has a relationship with Neutron Density / porosity difference, and the correlation coefficient is 0.76. The equation is:

$$V_{\text{clay\_ND}} = 4.81505 + 240.752 * \text{DIFFND})/100$$

Where

$$\text{DIFFND} = \text{NPHI} - \text{DPHI}$$

and,

$$\text{DPHI} = \frac{\text{RHOG} - \text{RHOB}}{\text{RHOG} - \text{RHOF}}$$

$V_{\text{clay\_ND}}$  = Clay volume, calculated from neutron density log, v/v

$\text{NPHI}$  = Neutron Limestone porosity, v/v

$\text{DPHI}$  = Density Limestone porosity, v/v

$\text{RHOG}$  = Limestone grain density, 2710 kg/m<sup>3</sup>

$\text{RHOB}$  = Bulk density from wireline log, kg/m<sup>3</sup>

$\text{RHOF}$  = Fluid (water) density, 1000 kg/m<sup>3</sup>

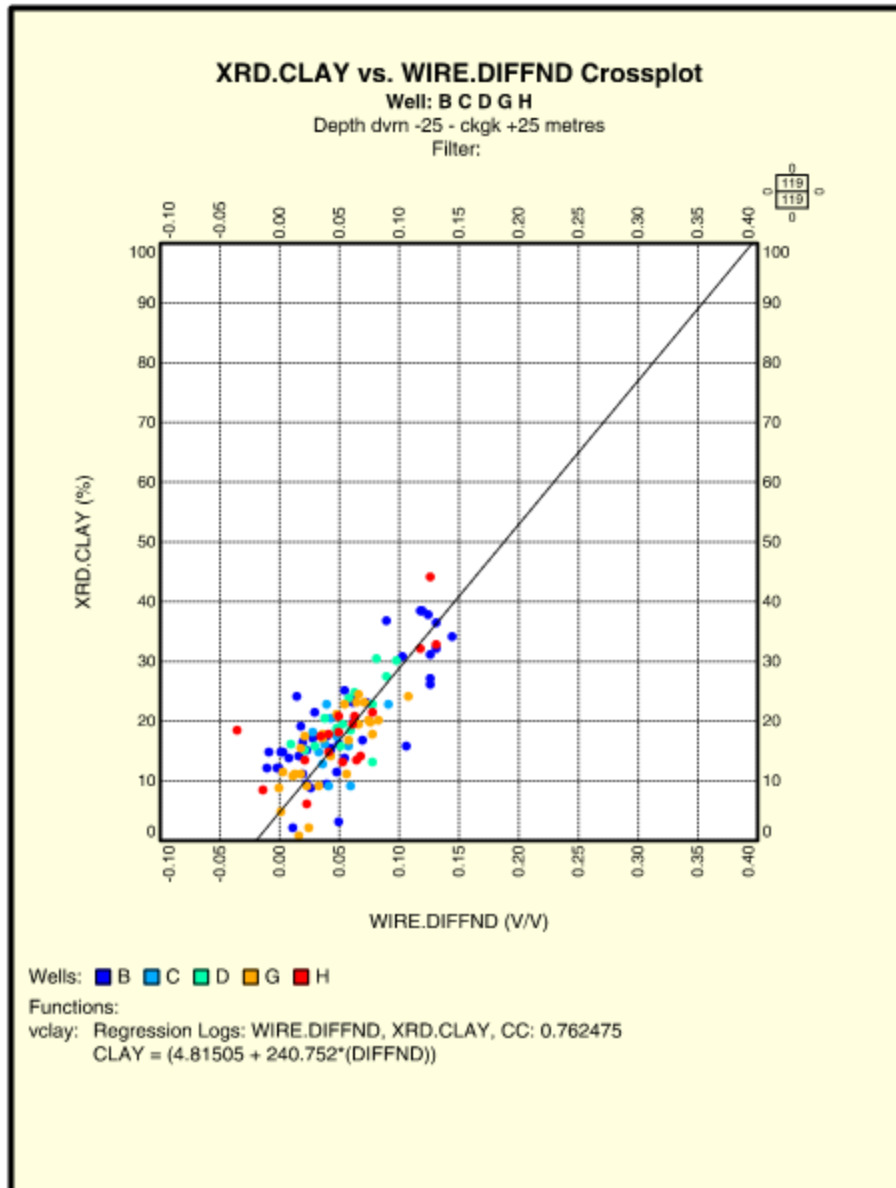


Figure 2.3.1 Clay vs. DIFFND cross plot

Clay volume is also calculated from gamma ray (GR), as Figure 2.3.2. The GR derived clay volumes should be similar to the neutron density derivation method in a non-organic shale zone, which can be used as quality control.

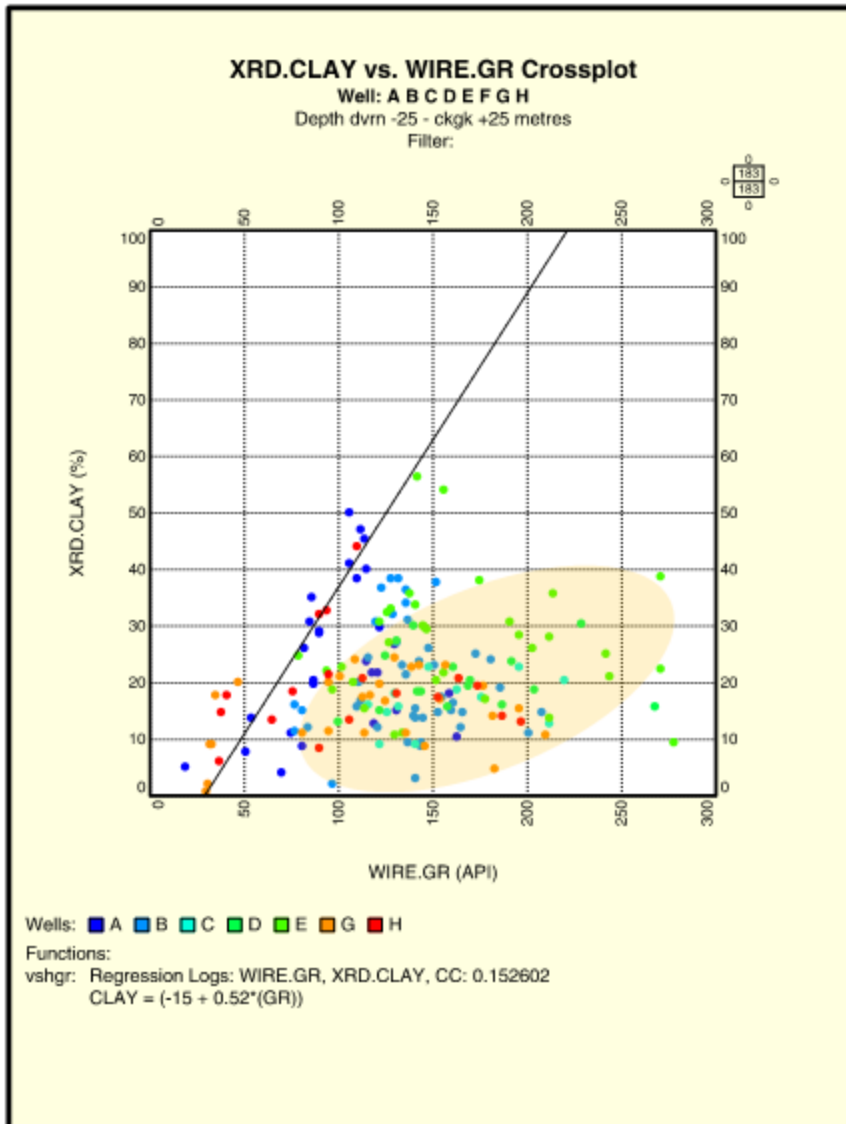


Figure 2.3.2 Clay vs. GR cross plot

$$V_{clay_{GR}} = \frac{0.52 * GR - 15}{100}$$

$V_{clay_{GR}}$  = Clay volume, calculated from gamma ray log, v/v

GR = gamma ray log, API

The final clay volume is determined by the minimum of the  $V_{clay}$  from those two methods.

### 2.3.2 Porosity

Comparing normal sedimentary rocks, organic matter in the unconventional play has low density and high hydrogen component; therefore, the wireline log responses have high neutron and a low density reading. The direct calculated apparent porosity from the neutron/density method will give a much higher result than the real number in the unconventional reservoir.

In this situation, the total porosity can be determined either from organic matter corrected porosity, or derived from variable grain density. Considering it is hard to verify the organic matters' density with limited data resource, variable grain density is more obtainable.

With A, B, C, D wells, log RHOB (bulk density) and DIFFND (porosity difference between neutron limestone porosity and density limestone porosity, v/v) have been used to perform the multiple regression, and build the relationship with core grain density RHOG (kg/m<sup>3</sup>). The regression equation as:

$$\text{RHOG} = (1363.563 + 0.497005*(\text{RHOB}) + 277.27*(\text{DIFFND}))$$

Where

$$\text{DIFFND} = \text{NPHI} - \text{DPHI}$$

and,

$$\text{DPHI} = \frac{\text{RHOG} - \text{RHOB}}{\text{RHOG} - \text{RHOF}}$$

RHOG = Calculated Grain density, kg/m<sup>3</sup>

RHOB = Bulk density from wireline log, kg/m<sup>3</sup>

NPHI = Neutron Limestone porosity, v/v

DPHI = Density Limestone porosity, v/v

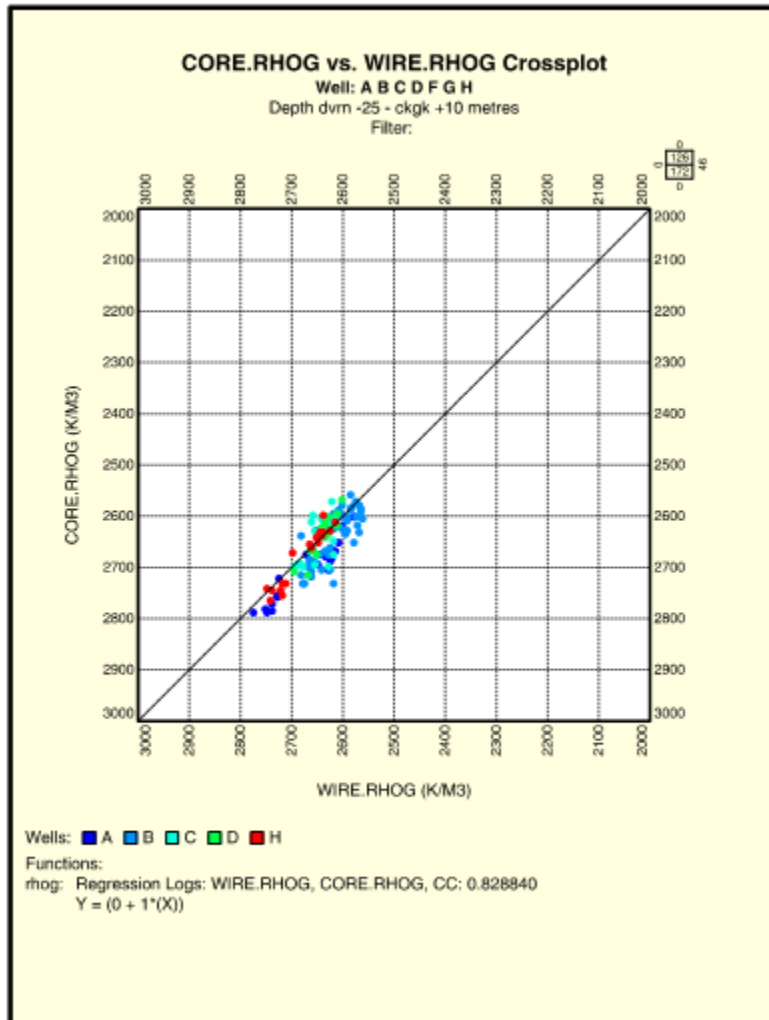


Figure 2.3.3 Core Grain Density vs. Log Derived Grain Density

Neither of the individual logs (RHOB and DIFFND) have a very high correlation and coefficient with grain density (RHOG), these being only 0.576 and 0.136; however, Figure 2.3.3 shows Core to Log derived grain density correlation coefficient is relatively high, at 0.828.

The total porosity can be calculated from :

$$\text{Phit} = \frac{\text{RHOG} - \text{RHOB}}{\text{RHOG} - \text{RHOF}}$$

- Phit = Total porosity, v/v
- RHOG = Calculated grain density, kg/m<sup>3</sup>
- RHOB = Bulk density from wireline log, kg/m<sup>3</sup>
- RHOF = Fluid density, kg/m<sup>3</sup>

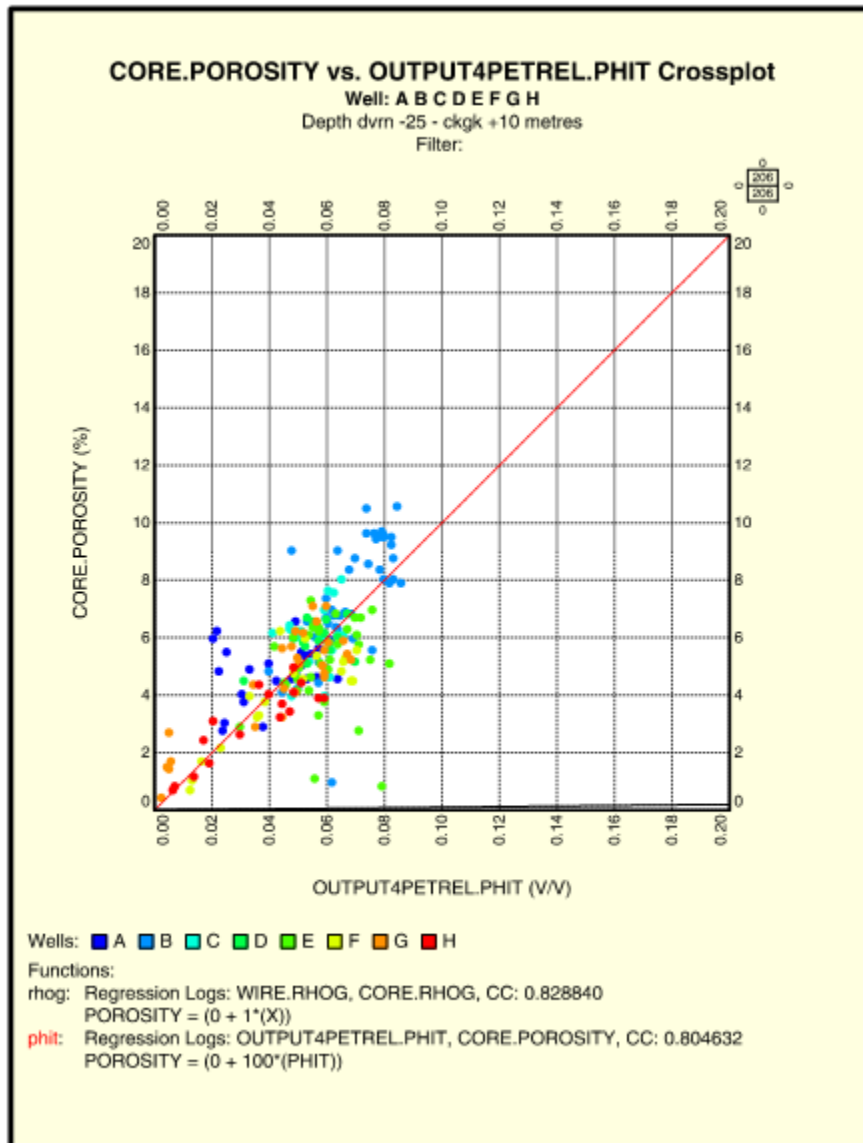


Figure 2.3.4 Core porosity vs. Log derived porosity

The comparison of Core porosity to log derived porosity (Figure 2.3.4), shows a close relationship between them (correlation coefficient: 0.80); however, in Figure 2.3.5, well G shows a different trend, in which Log calculated porosity is about 2% higher than the core porosity.

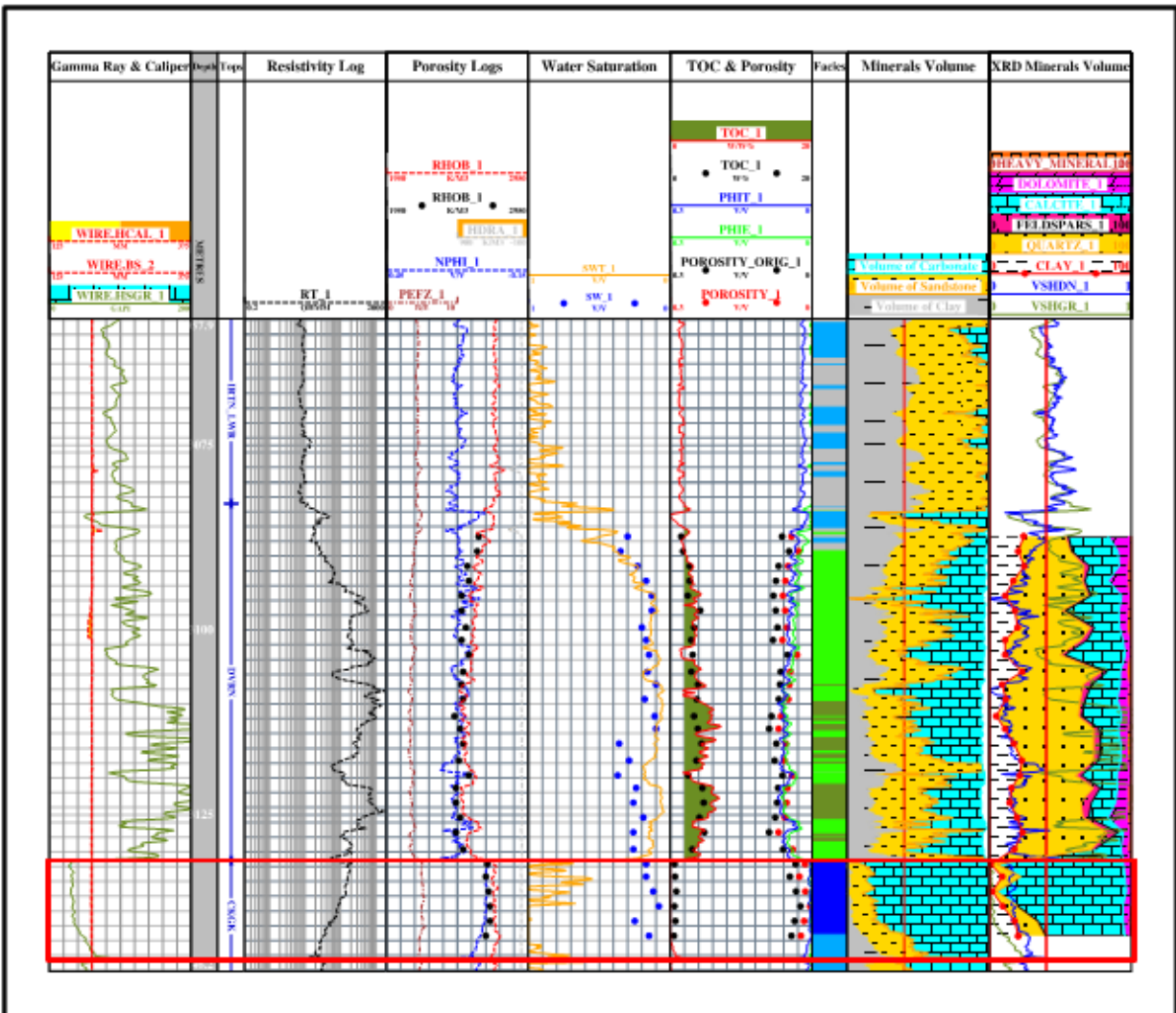
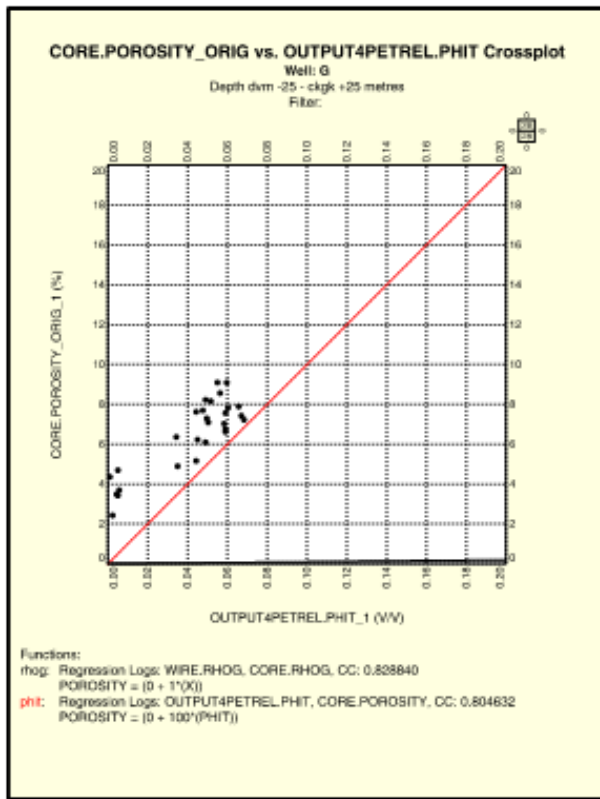


Figure 2.3.5 well G logs layout

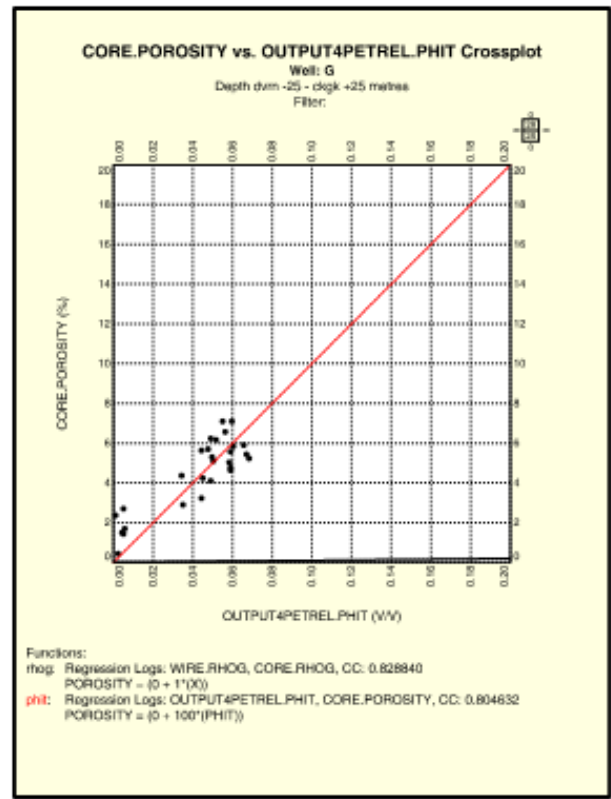
In the red rectangle zone in Figure 2.3.5 (the first digital number has been substituted by x for confidentiality reason), the neutron limestone porosity reading (blue curve in the Porosity Log track) is about 0%, the Bulk Density - RHOB (red curve in the

same track) is about 2.71, and the PE curve (brown curve in the same track) is around 5, which is a typical log response of limestone with close to 0 porosity, which agree with the log calculated porosity (PHIT, blue curve in the TOC & Porosity track).

However, the core analysis data (POROSITY\_ORIG, black dots in the TOC & Porosity track) are all higher than the log calculated porosity PHIT (blue curve in the same track); as a comparison, the after correction core porosity (original core porosity minus 2%, red dots in the TOC & Porosity track) seem more reasonable.



a



b

Figure 2.3.6 well G core porosity vs. Log derived porosity

Figure 2.3.6 graph a shows the well G core porosity data points are away from the trend line. After 2% porosity decrease, Figure 2.3.6 graph b core porosity is a better match with the log porosity, which was derived from other wells core to log relationship.

### 2.3.3 Water Saturation

The Archie equation is used for deriving water saturation in the Duvernay area.

G. E. Archie published a paper named “The Electrical Resistivity Log as an Aid in Determining Some Reservoir Characteristics” in 1942, in which  $S_{WT}$  can be calculated from rock porosity, connate-water resistivity, and several rock electrical properties.

The key experimental equation (Archie, 1942) could be written as:

$$S_{WT}^n = \frac{R_W \times a}{R_T \times \Phi^m}$$

Where,

$S_{WT}$  = total water saturation, v/v

$n$  = Archie saturation exponent

$R_W$  = connate-brine resistivity, ohm.m

$a$  = Archie cementation constant

$R_T$  = true formation resistivity (log resistivity), ohm.m

$\Phi$  = porosity (phit), v/v

$m$  = Archie cementation exponent

In Archie’s equation, cementation constant “ $a$ ” is set to 1; formation resistivity  $R_T$  is from log deep resistivity; connate-brine resistivity  $R_W$  is from local experimental water salinity; and the porosity  $\Phi$  (total porosity, PHIT) is from previous calculation. The rest of parameters,  $m$  and  $n$ , need to be resolved, since they are not available from the public resources. The Pickett plot (Pickett, 1973) provides a way to estimate the  $m$  and  $n$  range in this case.

The Pickett plot uses a double logarithmic (to base ten) scale graphic crossplot of the porosity and resistivity, as Figure 2.3.7.

In the Pickett plot,  $R_w$  has been used as 0.05 ohm.m based on area experience, shown as the red star at the top left corner in the Figure 2.3.6. This point represents 100% water saturation with 100% porosity. Through this point, a line can be drawn along the left outline of points' cluster, which is the 100% water line. The points under the shaded area with low porosity (less than 2%) do not belong to the discussed organic rich zone.

The Archie cementation exponent  $m$  is determined by the slope of the line. As Figure 2.3.7 shows,  $m$  could be adjusted to change the slope angle to fit in the target zone data points. The slope of the trend line is  $m = 1.7$  in this case. Changing the line slope could result in a different  $m$ . As illustrated in Figure 2.3.8, the slope trend goes away from the left edge of the data cloud as  $m = 1.2$  in graph a, and  $m = 2$  in graph b.

The Archie saturation exponent  $n$  can also be decided by the Pickett plot. As other parameters have been set up, the paralleled line with different water saturation can be drawn, as water saturation equal to 100%, 75%, 50%, 25%, and 10%, as Figure 2.3.7. Through adjusting  $n$ , those lines can be squeezed and stretched, to fit all the data. In this example data set,  $n$  is about 2.4. As Figure 2.3.9 shows, the data points cannot be covered between 100% and 10% water saturation lines when  $n$  equals to 2 in graph a, and it is beyond the data range when  $n$  equals to 3 in graph b.

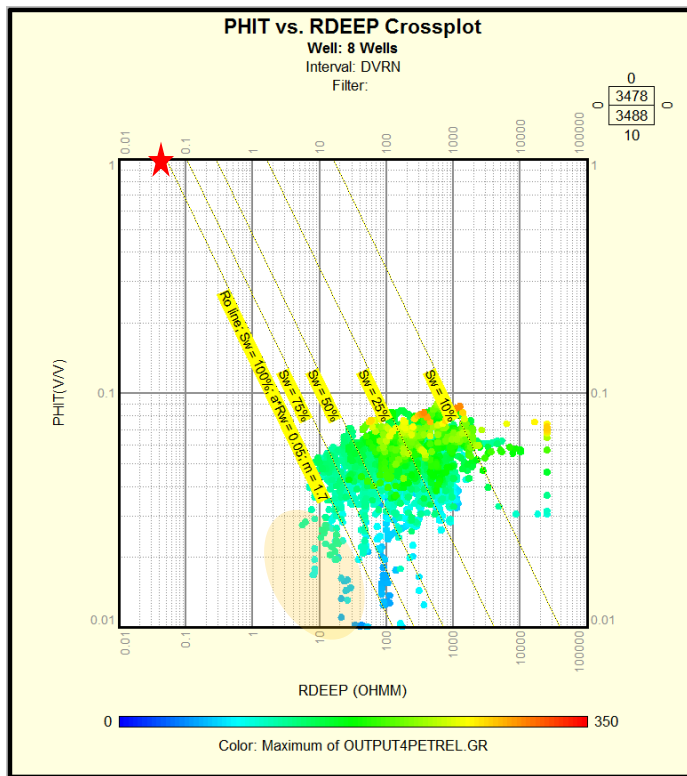
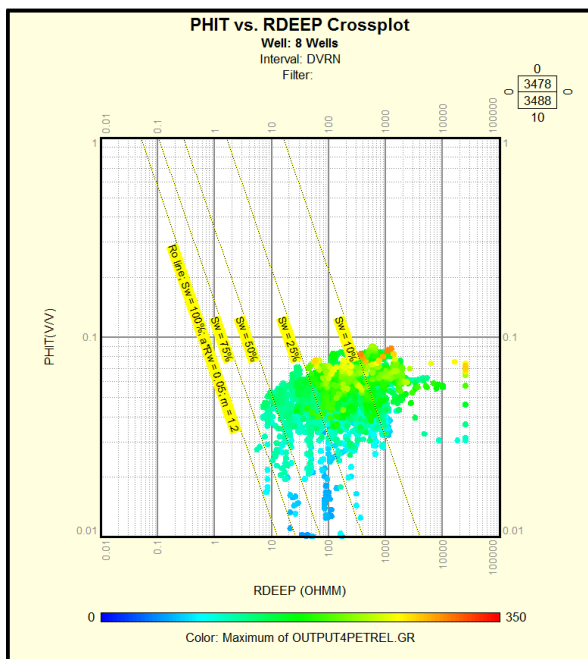
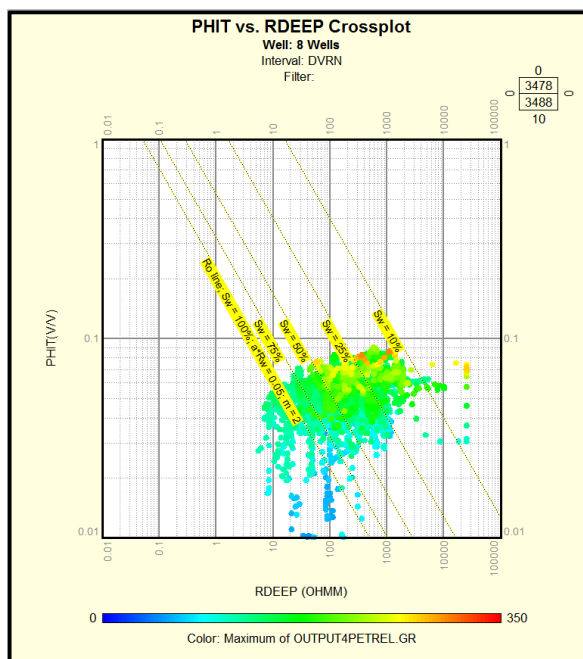


Figure 2.3.7 Pickett plot ( $m=1.7$ ,  $n=2.4$ )

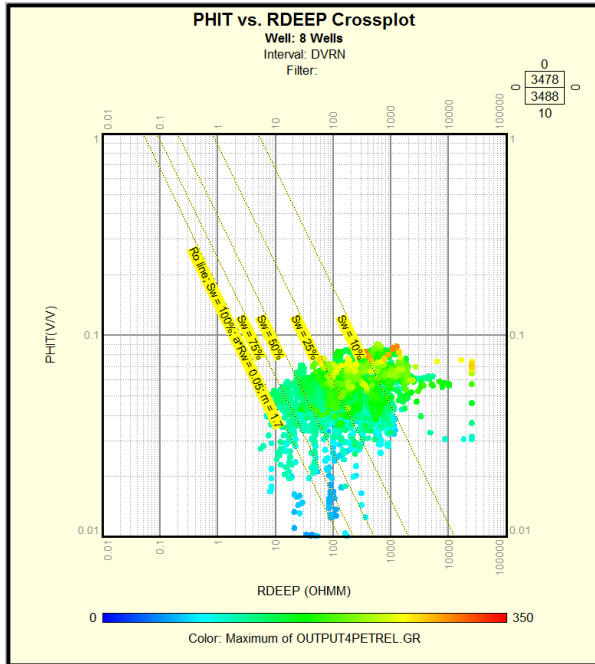


a.  $m=1.2$

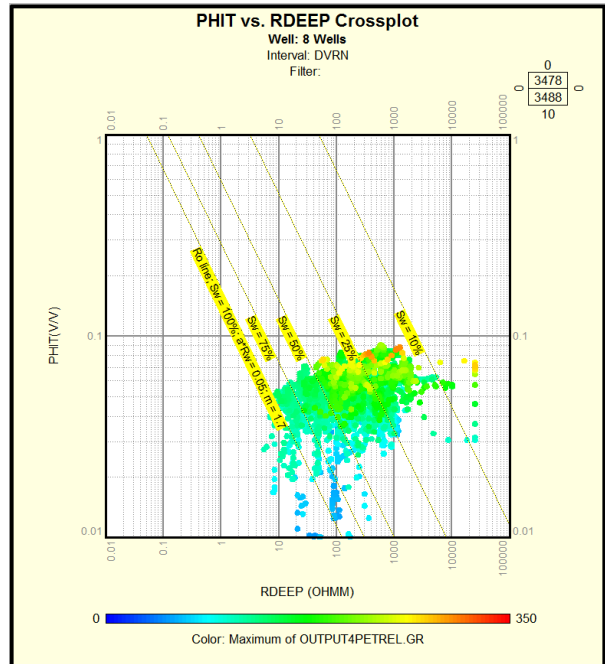


b.  $m=2$

Figure 2.3.8 Pickett plot with different slope angle (different  $m$ )



a. n=2



b. n=3

Figure 2.3.9 Pickett plot with different n

### 2.3.4 Total organic carbon

The TOC (total organic carbon) computed from Delta Log R method was first discussed by Passey et al. (1990), and the basic method involves computing the difference of linear scale porosity log curve to the logarithmic scale resistivity log curve.

The methodology is to overlay sonic log and resistivity log at “non-source” places, and treat the overlying place sonic and resistivity reading as the base lines, as Figure 2.3.10; then, the red envelope area (called Delta Log R or  $\Delta\text{LogR}$ ) are either source rock or resource. In the mature source place, as the middle part of Figure 2.3.8, the Delta Log R is related to TOC (total organic carbon).

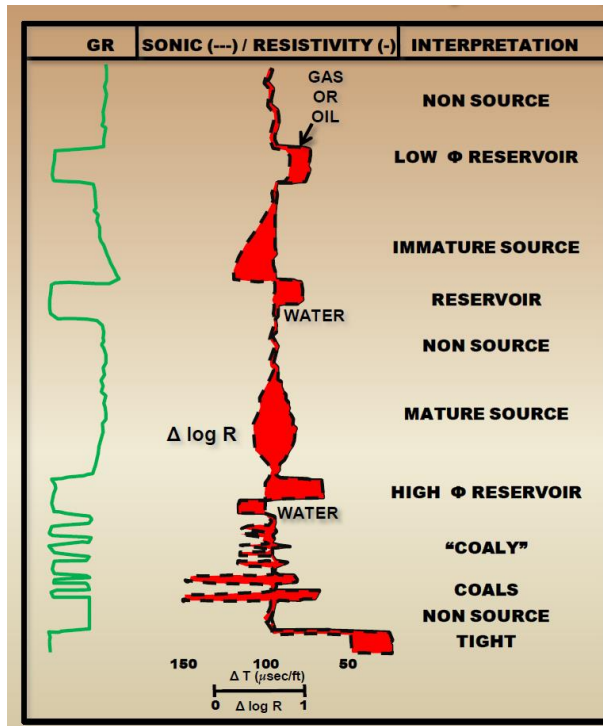


Figure 2.3.10 Schematic guide of Delta Log R response (from Bowman T., 2010, after Passey et al. 1990)

As Figure 2.3.10 is showing, Delta Log R has cross over at the mature source place, which occurs clearly in the Duvernay TOC rich zone.

Since the density log is one of the minimum study requirements for the target area, the density – resistivity overlay is used to derive  $\Delta \log R$ , shown in Figure 2.3.11, as the yellow filled area in the right track.

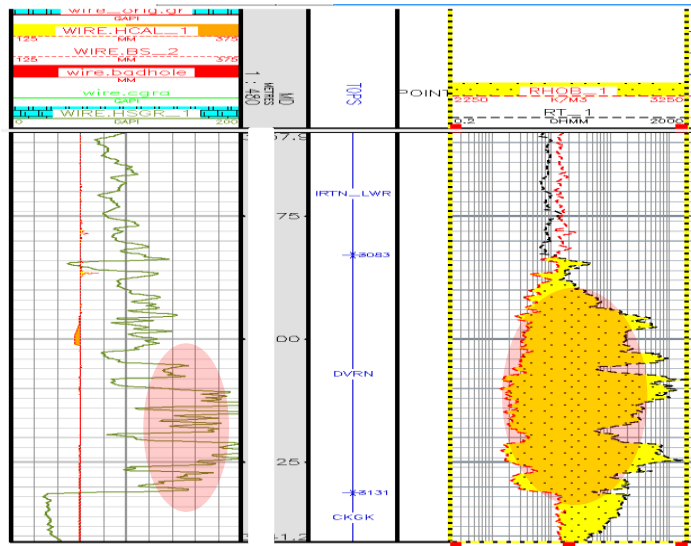


Figure 2.3.11 Delta Log R method applied to Density-Resistivity logs

$$\Delta\text{LogR} = \text{Log}_{10} \left( \frac{R_T}{R_{T\text{baseline}}} \right) + (P * (\Phi_D - \Phi_{D\text{baseline}}))$$

P = times factor

$\Phi_D$  = density porosity limestone

$\Phi_{D\text{baseline}}$  = density porosity limestone baseline reading to non-source place

$R_T$  = resistivity

$R_{T\text{baseline}}$  = resistivity baseline reading at non-source place

$$\text{TOC}_{\Delta\text{LogR}} = \text{TOC}_{\text{baseline}} + \Delta\text{LogR} * 10^{(2.297-0.1688*\text{LOM})} * c$$

$\text{TOC}_{\Delta\text{LogR}}$  = total organic carbon from  $\Delta\text{LogR}$  method

LOM = level of Maturity

c = adjust factor

Passey had suggested this method as a better alternative for LOM (Level of Maturity) between 6-12. In the equation, the level of maturity is derived from:

$$\text{LOM} = 5.75 * \ln(\text{Vro}) + 9.9$$

Vro = Vitrinite Reflectance

“The relatively high natural radioactivity of organic-rich shale has already been discussed in some detail”, as Fertl and Chillingar 1990 suggested, GR log could be used to determine TOC directly.

For Duvernay Kaybob area, TOC also can be calculated from gamma ray, as:

$$\text{TOC}_{\text{GR}} = \frac{\text{GR}-50}{450-50} \times 20$$

TOC<sub>GR</sub> = total organic carbon from gamma ray method

The final TOC is from:

$$\text{TOC} = (\text{TOC}_{\Delta\text{LogR}} + \text{TOC}_{\text{GR}}) / 2$$

As long as either TOC<sub>ΔLogR</sub> or TOC<sub>GR</sub> is lower than 1%, the TOC will be equal to the lower one. Combining the two methods can avoid some misleading TOC results (TOC in Carbonate zone with high resistivity with ΔLogR method, or not real TOC with GR method in clay rich zone).

## 2.4 The petrophysical model to core comparison

The core based petrophysical model is applied to all eight cored wells, to visually compare if the log derived results agree with the core. Figure 2.4.1 to Figure 2.4.8 are final layouts. All the dots represent core samples, and lines are either wireline logs or logs calculated results. The layout details from left to right as following:

### 1. Gamma Ray and Caliper

- GR, dark green line, gamma ray log, scale from 0 to 200 API unit

- CAL, orange dash line, caliper log, scale from 125 to 375 mm; shaded yellow if it is greater than bit size, shaded orange if it is less than bit size
2. Depth
- Measure depth in meters; first number has been hidden for confidentiality purpose
3. Tops
- Geologist picked tops, includes Ireton lower, Duvernay, and Cooking Lake (or Majeau Lake in some areas) in the layout covered interval.
4. Resistivity Logs
- RT, deep resistivity, logarithmic scale 0.2 to 2000 ohm.m
5. Porosity Logs
- PEF, brown line, photoelectric absorption factor, scale 0 – 10 BE at the left half track
  - NPHI, blue dash line, neutron porosity limestone, scale from 0.45 to -0.15 v/v
  - RHOB, red dash line, bulk density, scale from 1.95 to 2.95 g/m<sup>3</sup>
  - RHOB, black dots, bulk density from core analysis, scale from 1.95 to 2.95 g/m<sup>3</sup>
6. Water Saturation
- SWT, yellow line, log calculated total water saturation, scale from 1 to 0 v/v
  - SW, blue dots, water saturation from core analysis, scale from 1 to 0 v/v
7. TOC and Porosity
- TOC, red line, log calculated total organic carbon, scale from 0 – 20 w%, shaded dark green for greater than 2 w%

- TOC, black dots, total organic carbon from core analysis, scale from 0 – 20 w%
- Phit, blue line, log calculated total porosity, scale from 0.3 to 0 v/v
- Phie, green line, log calculated effective porosity, scale from 0.3 – 0 v/v
- Porosity, black dots, porosity from core analysis, scaled from 0.3 – 0 v/v

#### 8. Facies

- Log facies, five facies in total: tight (cyan), good reservoir (dark green), reservoir (green), clay (grey), carbonate (dark blue)

#### 9. Minerals Volume

- Clay, log calculated, grey shaded area, scale from 0 to 1 v/v
- Sandstone, log calculated, yellow shaded area, scale from 0 to 1 v/v, accumulates to the previous log
- Carbonate, log calculated, blue shaded area, scale from 0 to 1 v/v, accumulates to the previous log
- Phie, white space, scale from 0 to 1 v/v

#### 10. XRD (X-ray Diffraction) Minerals Volume

- Illite, black dash line on white background, scale from 0 to 100w%
- Quartz, black dots on yellow background, scale from 0 to 100w%, accumulates to the previous log
- Feldspar, black cross on red background, scale from 0 to 100w%, accumulates to the previous log
- Limestone, cyan, scale from 0 to 100w%, accumulates to the previous log
- Dolomite, pink, scale from 0 to 100w%, accumulates to the previous log

- Heavy mineral, black dash line one red background, scale from 0 to 100w%, accumulates to the previous log

Figure 2.4.1 and Figure 2.4.2 show well A and B logs correlated to core points matching. In the “Porosity Logs” track, core RHOB (black dots) go along with log bulk density RHOB (red curve) trend, which means the core points are on the correct depth. Other core points match the log derived result as well.

Figure 2.4.3 and Figure 2.4.4 present the same trend, except in the pink shaded areas, where core water saturation is higher than the log calculated water saturation. For those two wells, the total porosity shows a very good match for both wells. With the reliable calculated porosity, plus similar or even higher Resistivity reading comparing to other cored wells, it should not be 25% - 40% water volume present in the system, log derived water saturation is more reasonable. Based on that assumption, the water saturation model is kept; however, the water saturation uncertainty needs to be considered for reserve calculation in the future.

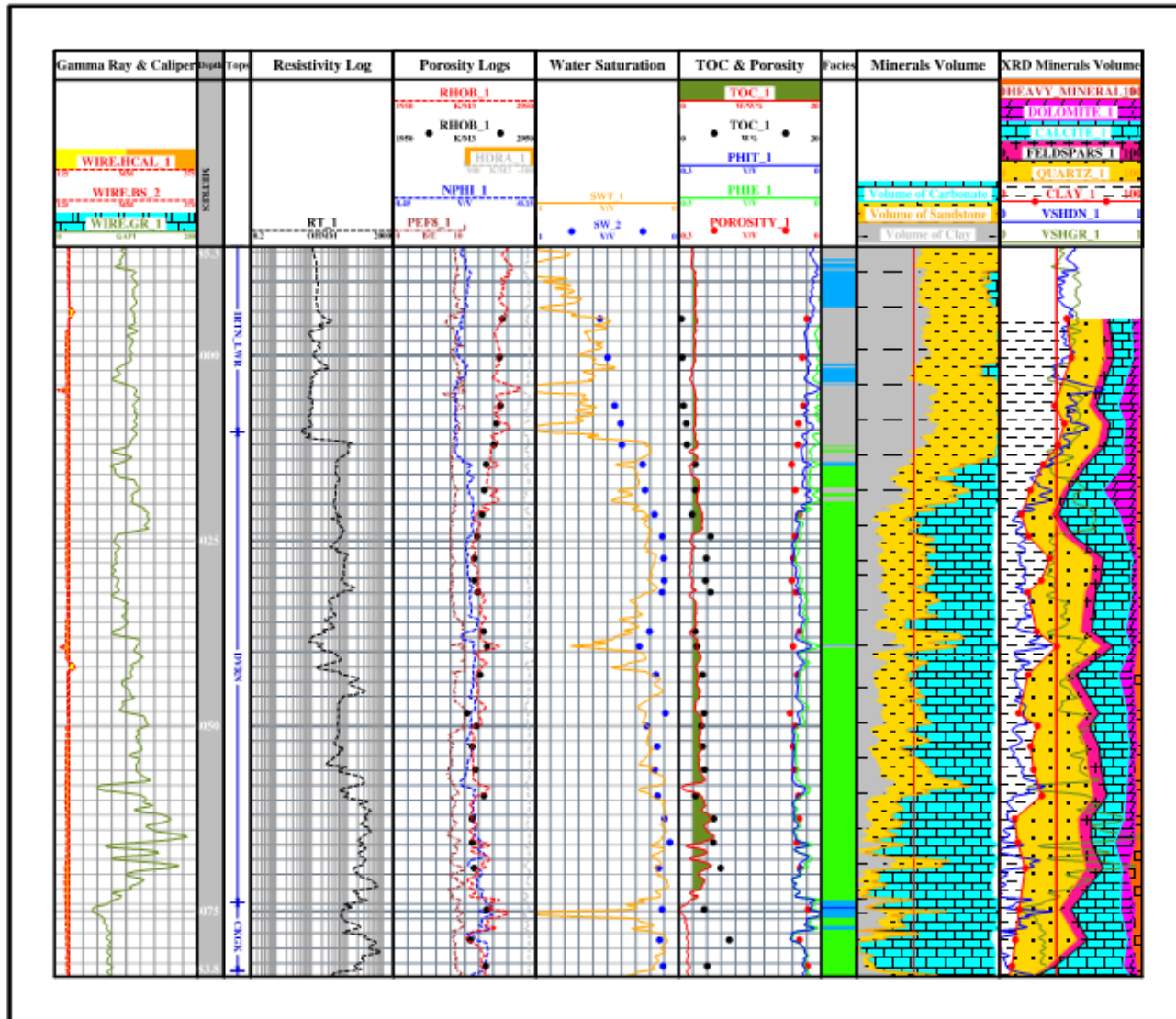


Figure 2.4.1 well A final layout

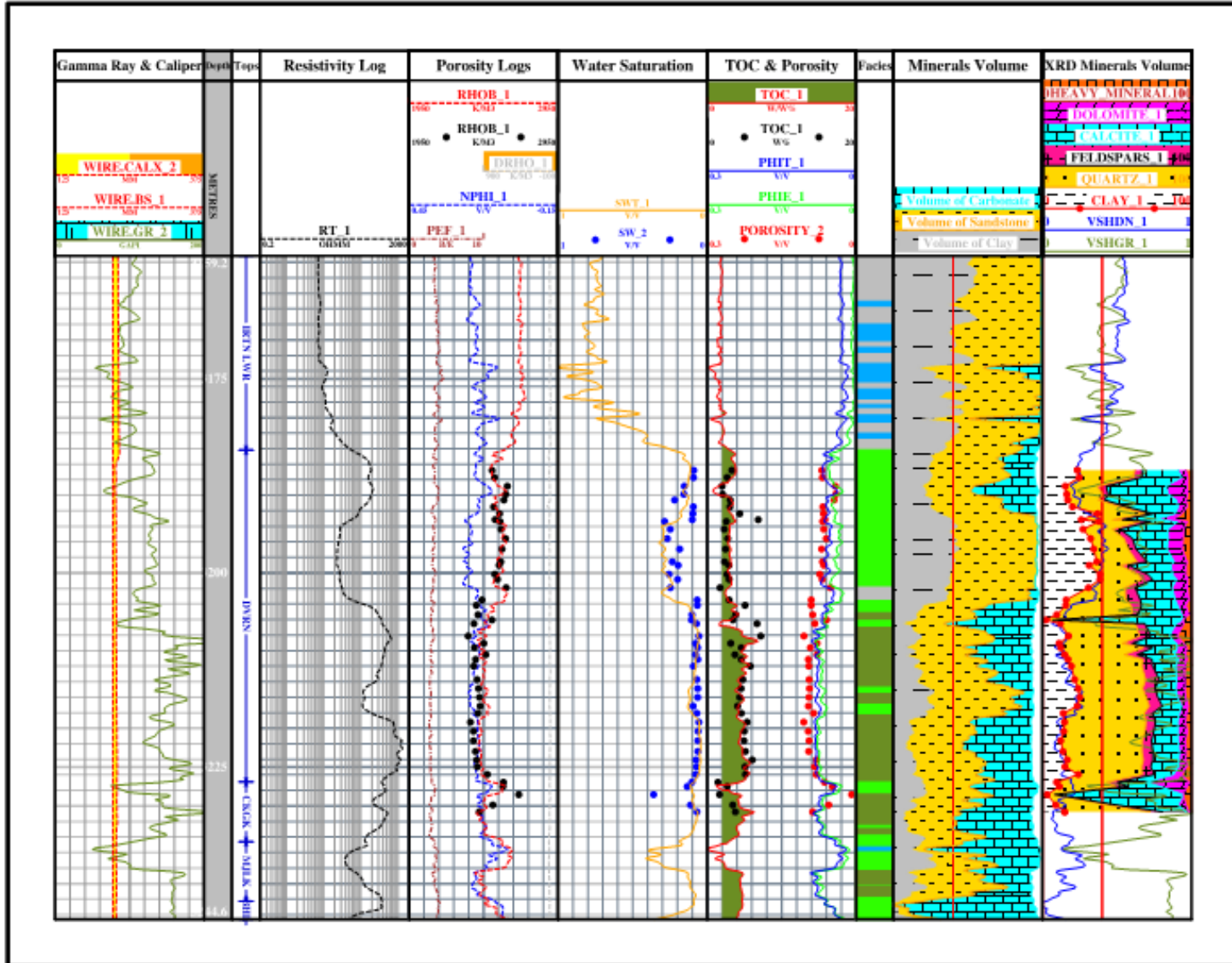


Figure 2.4.2 well B final layout

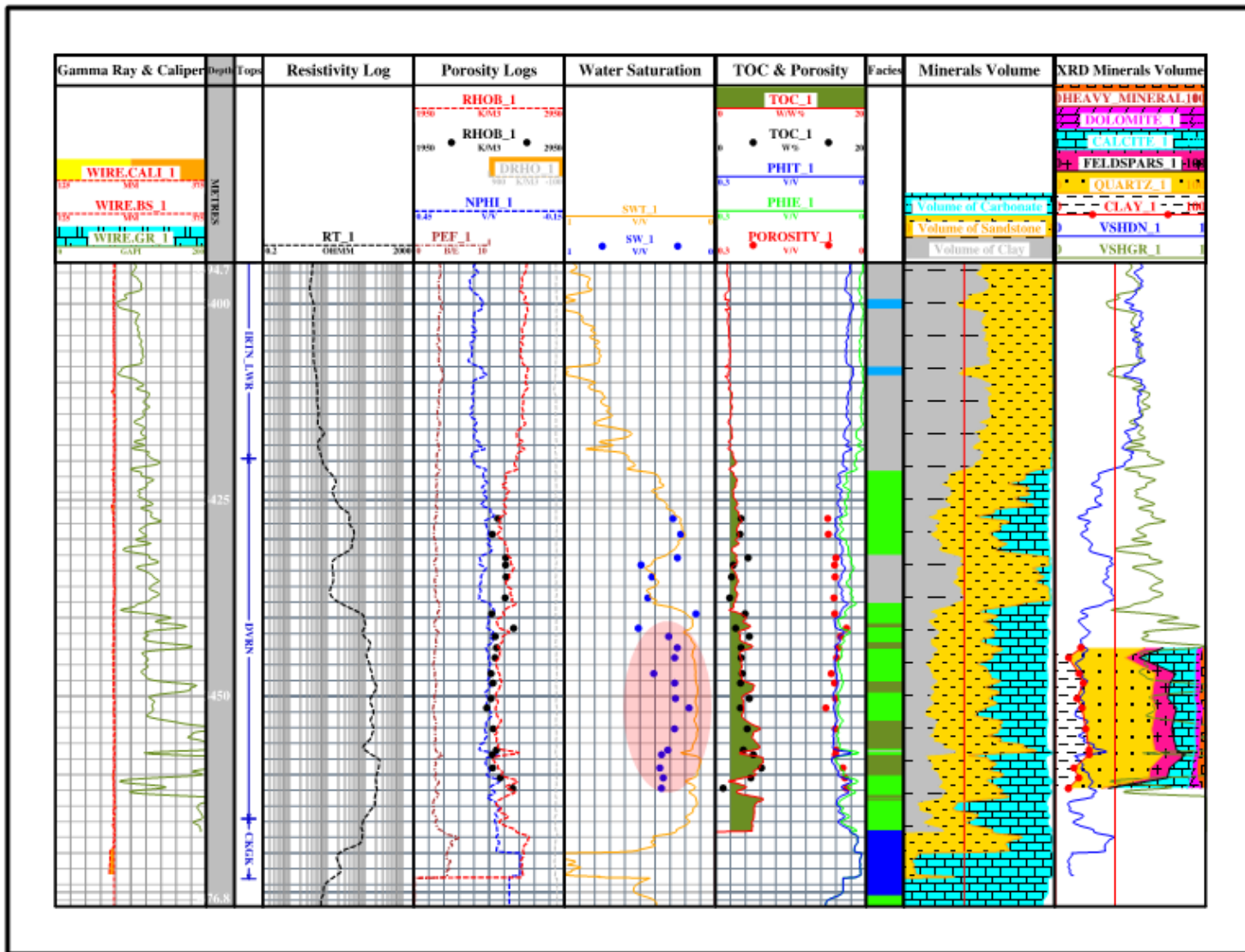


Figure 2.4.3 well C final layout

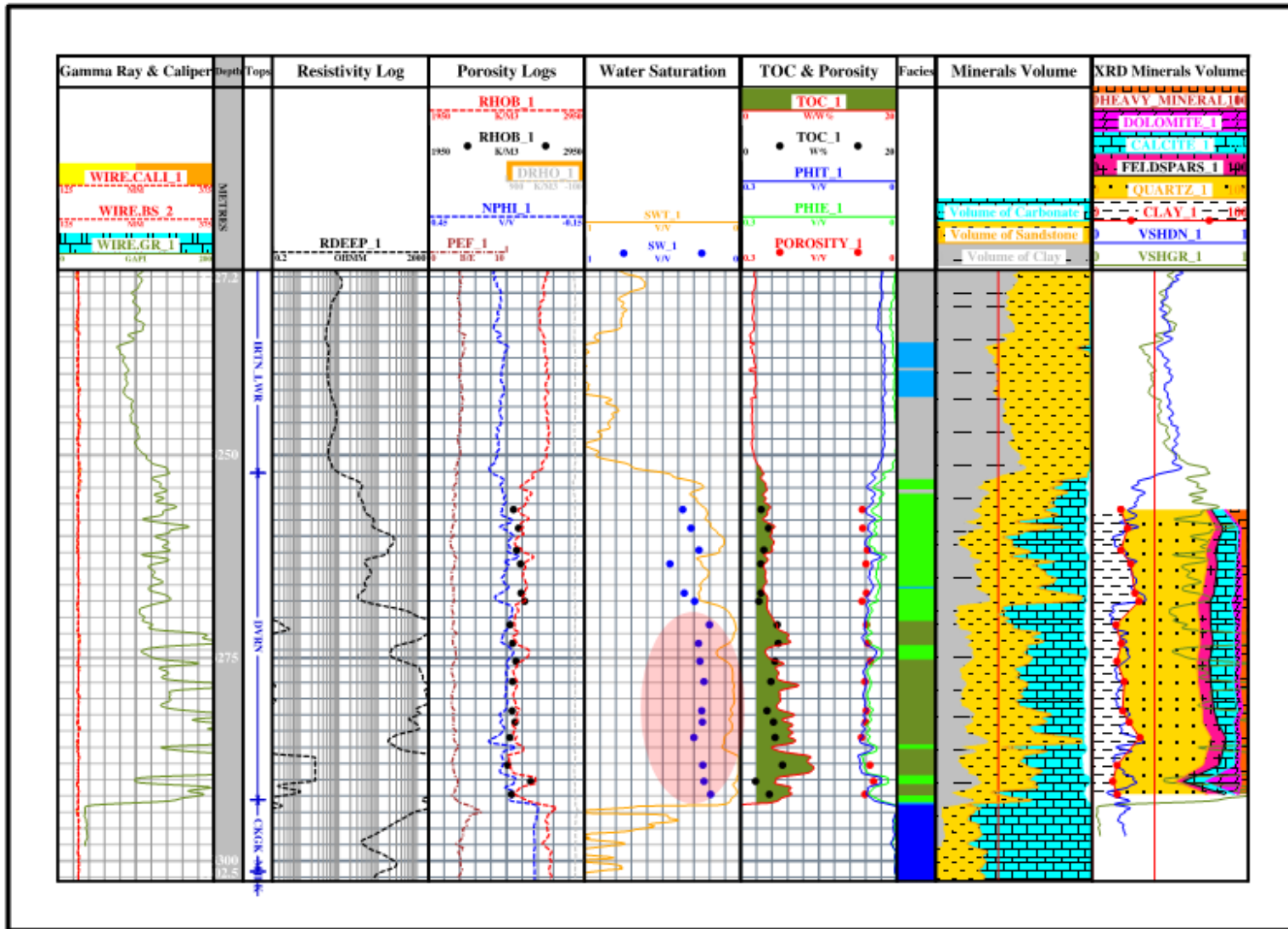


Figure 2.4.4 well D final layout

Figures 2.4.5 to 2.4.8 show the same trend, where core to log correlation are well matched.

At the pink shaded areas in well E, F, G, H (Figure 2.4.5 to Figure 2.4.8), calculated Swt (total water saturation) is higher than the core water saturation; however, those zones either belong to IRTN\_lwr or CKGK, that are outside of the study focusing zone of the Duvernay. I choose to ignore those parts, and focus on Duvernay only.

In summation, the comparison shows a very good correlation between core and log calculated results; therefore, the petrophysical model is reliable to calculate TOC, clay volume, porosity, and water saturation for non-cored wells.

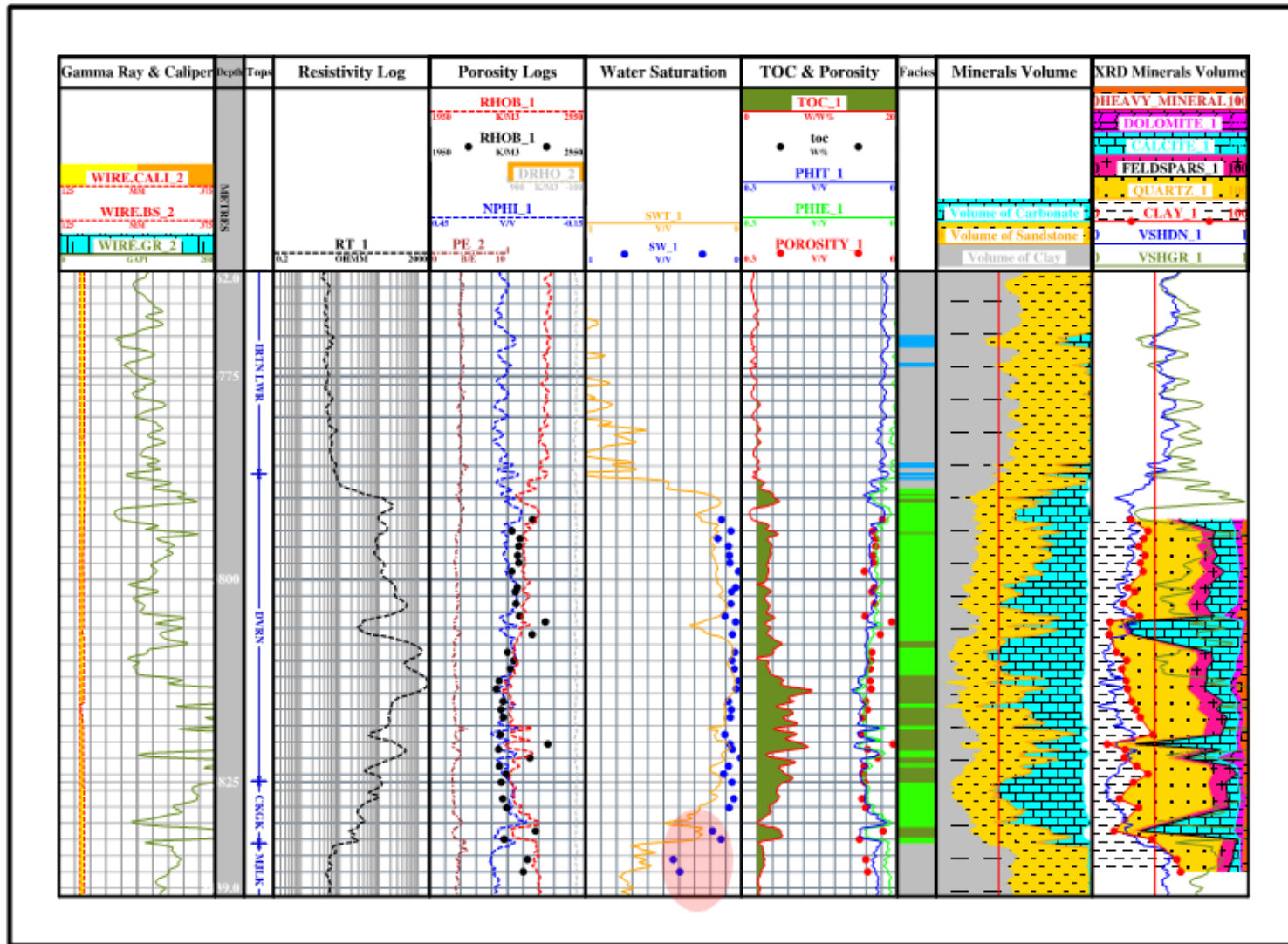


Figure 2.4.5 well E final layout

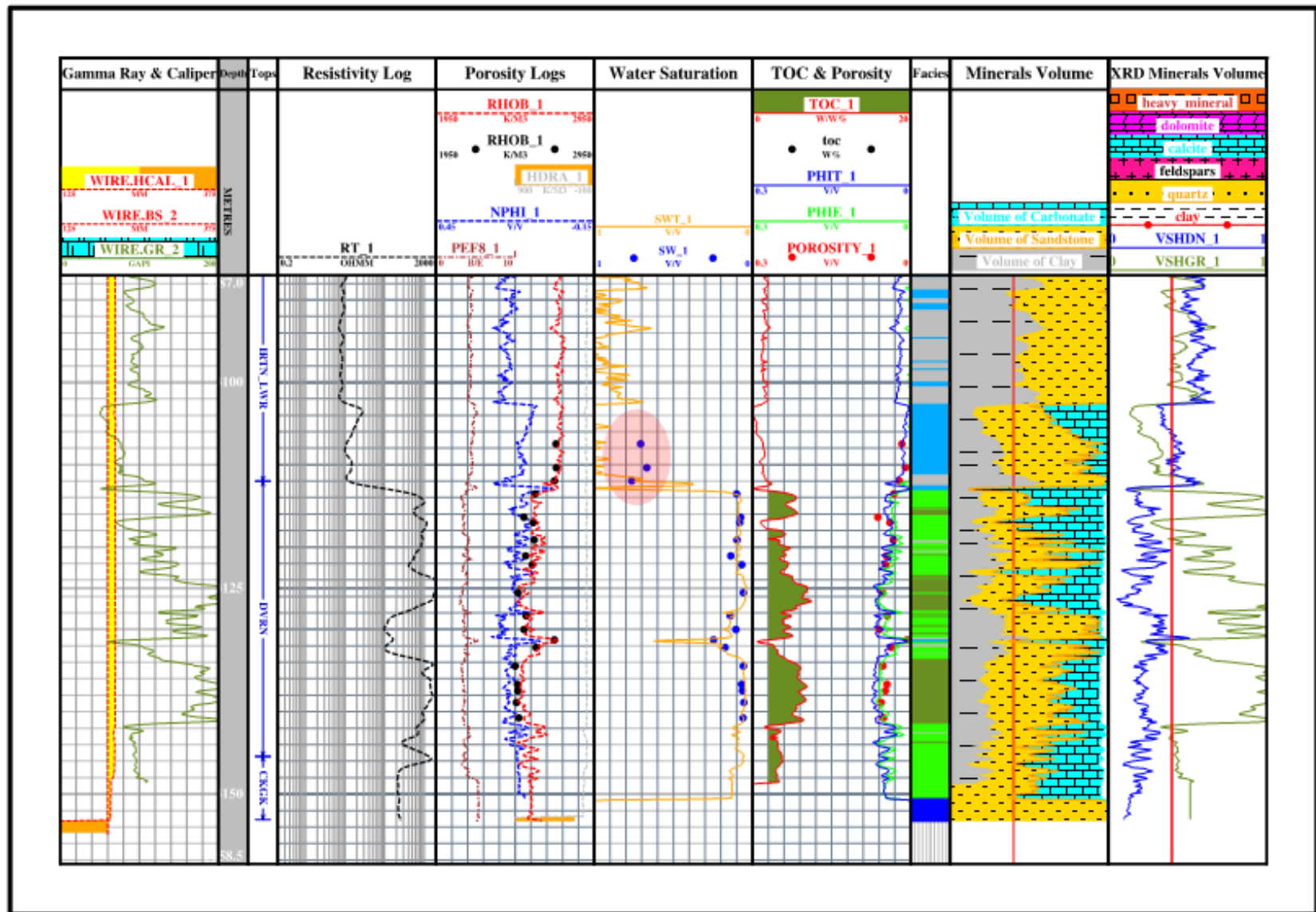


Figure 2.4.6 well F final layout

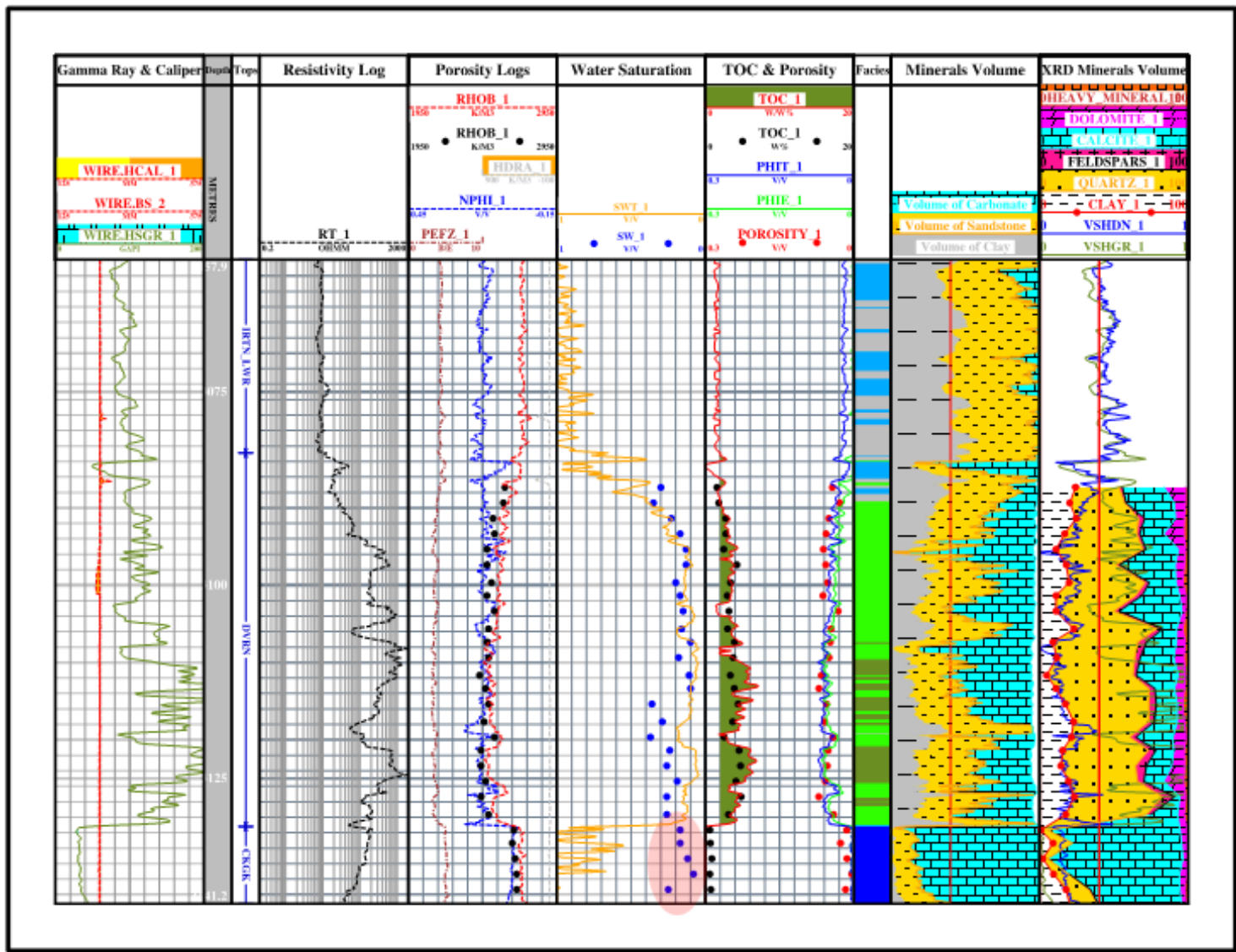


Figure 2.4.7 well G final layout

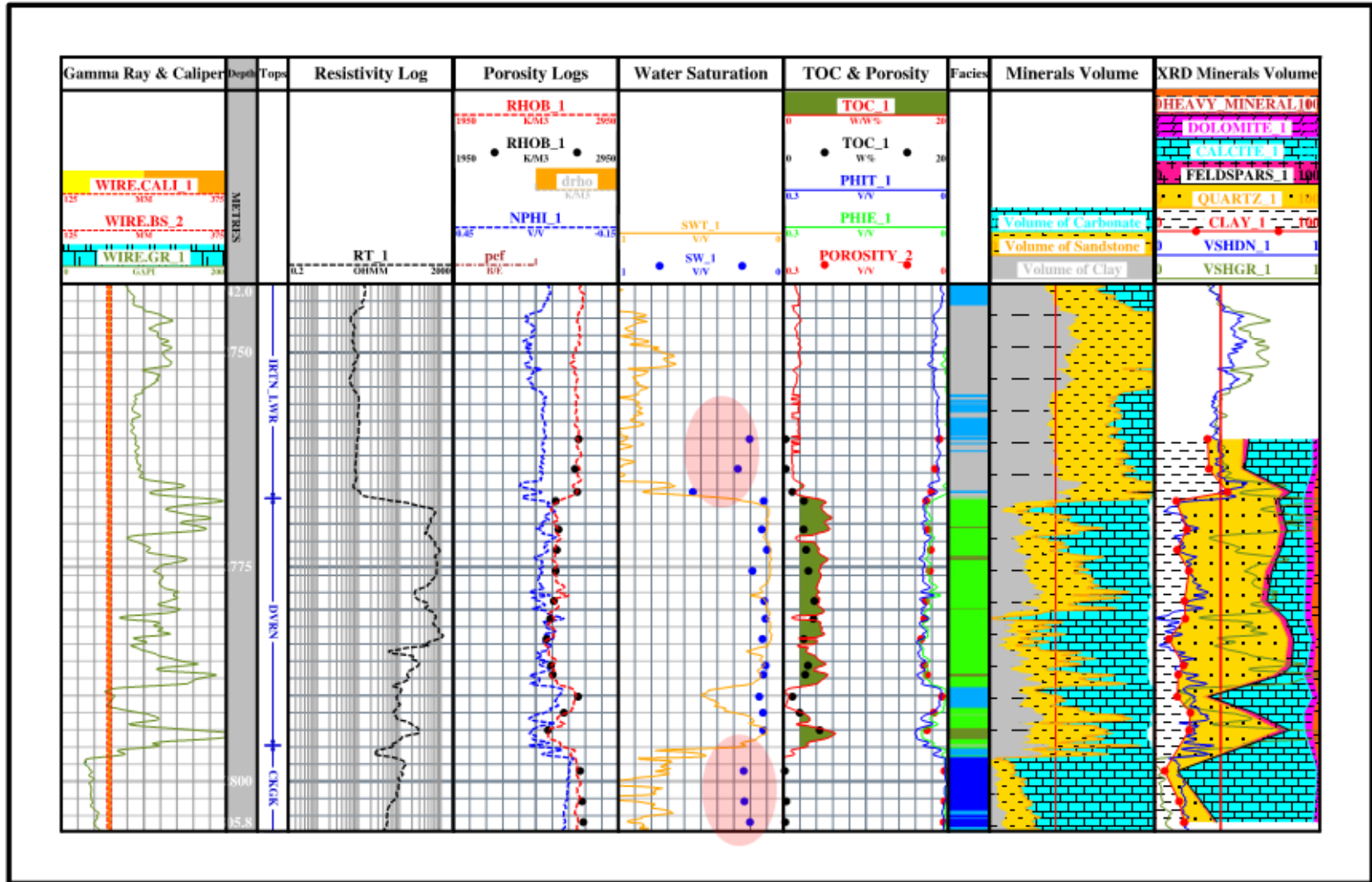


Figure 2.4.8 well H final layout

## 2.5 Result quality control

The common petrophysical data quality control procedure is to review every single well input logs and parameters, and compare the data distribution histogram to other wells with the similar deposition environment; then decide to do further normalization or standardization.

However, for exploration purposes, the working area is normally large, and the depositional environment could be variable. Though the normalization procedure could scale out the output, it blurs the description of the real environmental change. In addition, applying normalization to hundreds or thousands of wells is hard to achieve in a relatively tight time frame.

To solve this potential problem, the preliminary petrophysical results have been mapped out, using auto-mapping to get the data distribution and general trends. Through carefully checking the abnormal points, shown as three pink centered and blue surrounded areas in Figure 2.5.1 (color bar from 0 – 0.08), determinations confirming those are representative “true” numbers, or from a “bad data” were made.

Through this checking method, well I (Figure 2.5.2) was analyzed and it was discovered that porosity logs did not cover entire Duvernay interval, and so, the average porosity through full Duvernay zone gave a fake low number.

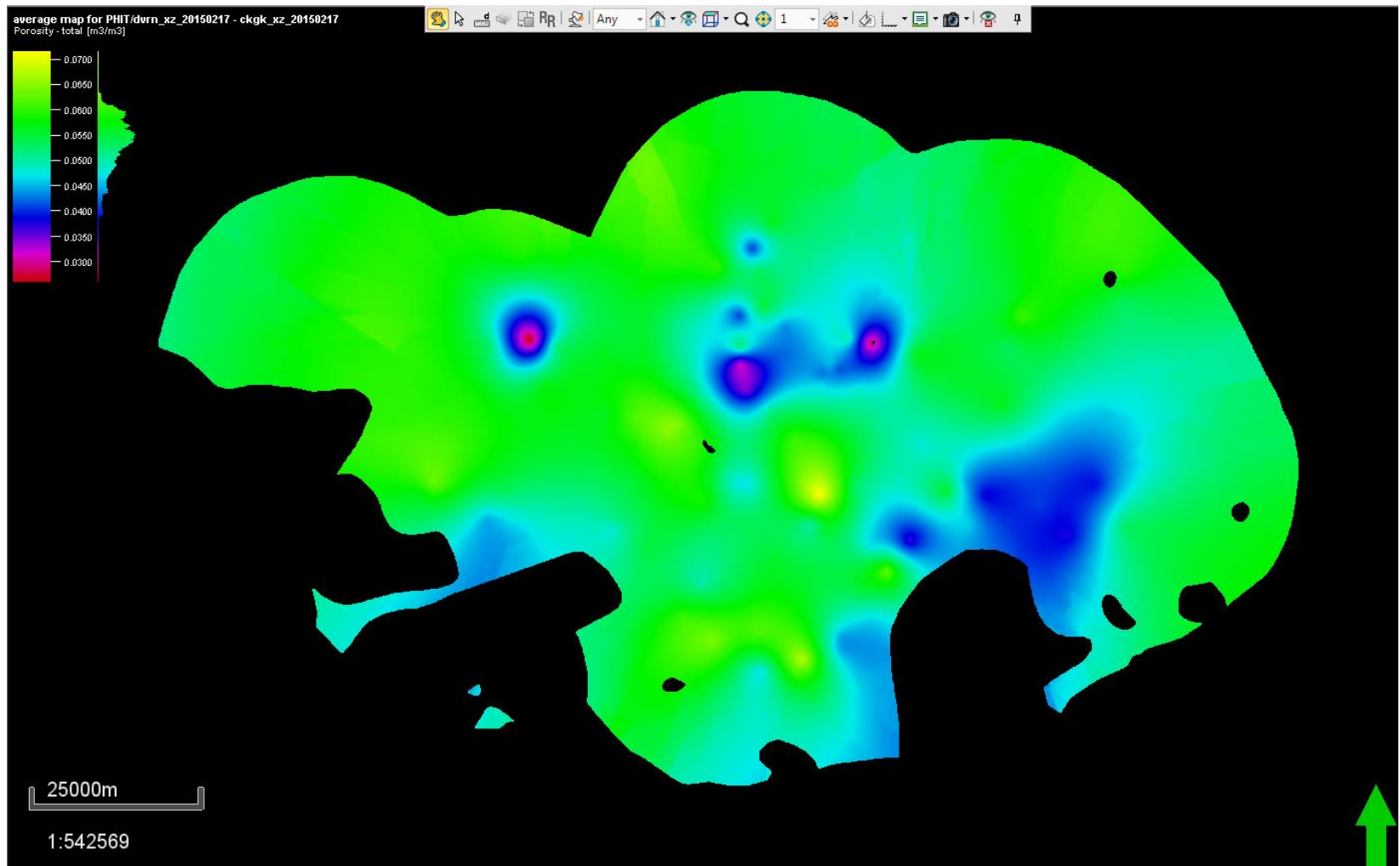


Figure 2.5.1 Preliminary porosity average plot

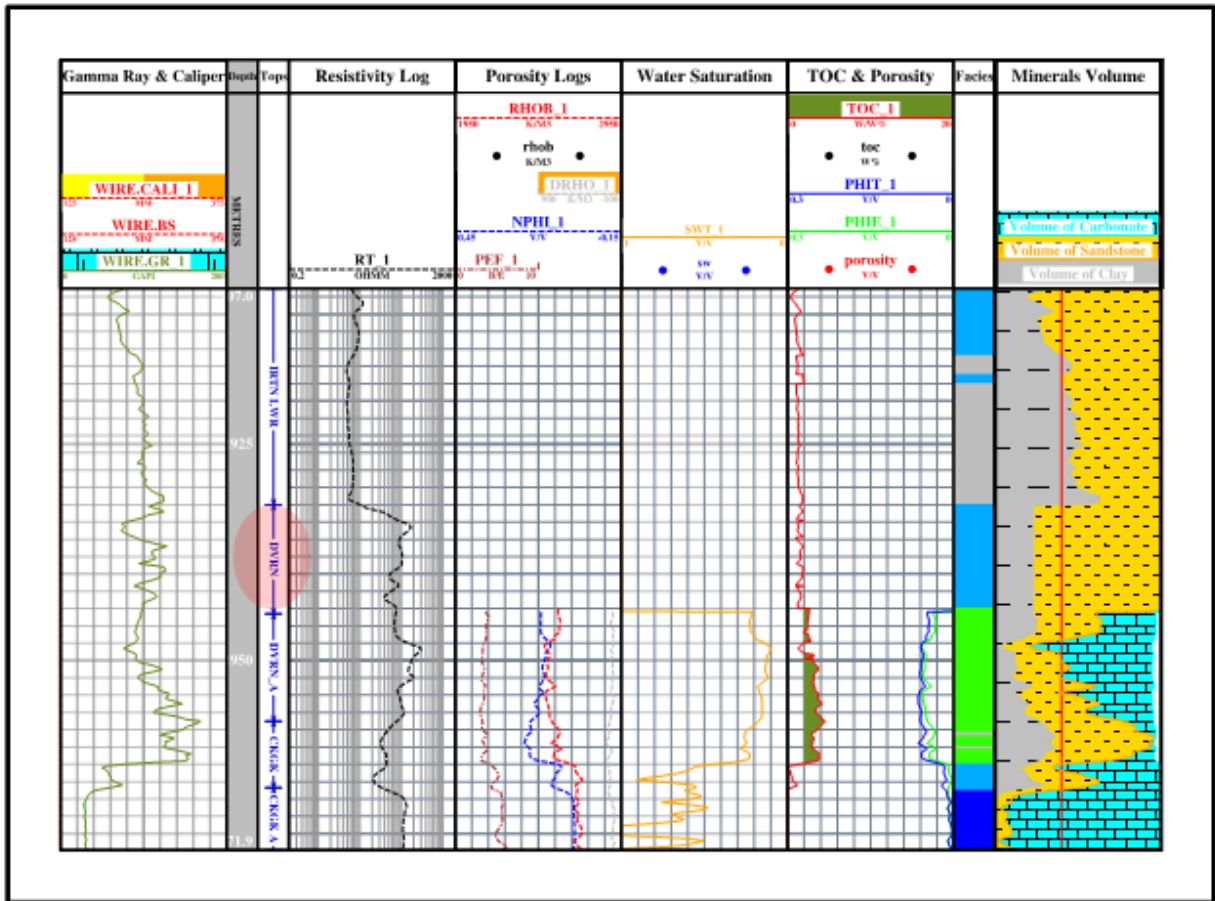


Figure 2.5.2 Well I plot

In two other anomalous points from the wells (Figure 2.5.3 as an example), the well J log data looks normal; however, through checking back the tops in Petrel, the loaded DVRN top was higher than the current point, into IRTN\_Lwr. Due to the low porosity in IRTN\_lwr, the average porosity had been pulled down.

After correcting the anomalous points, the final result is more reliable.

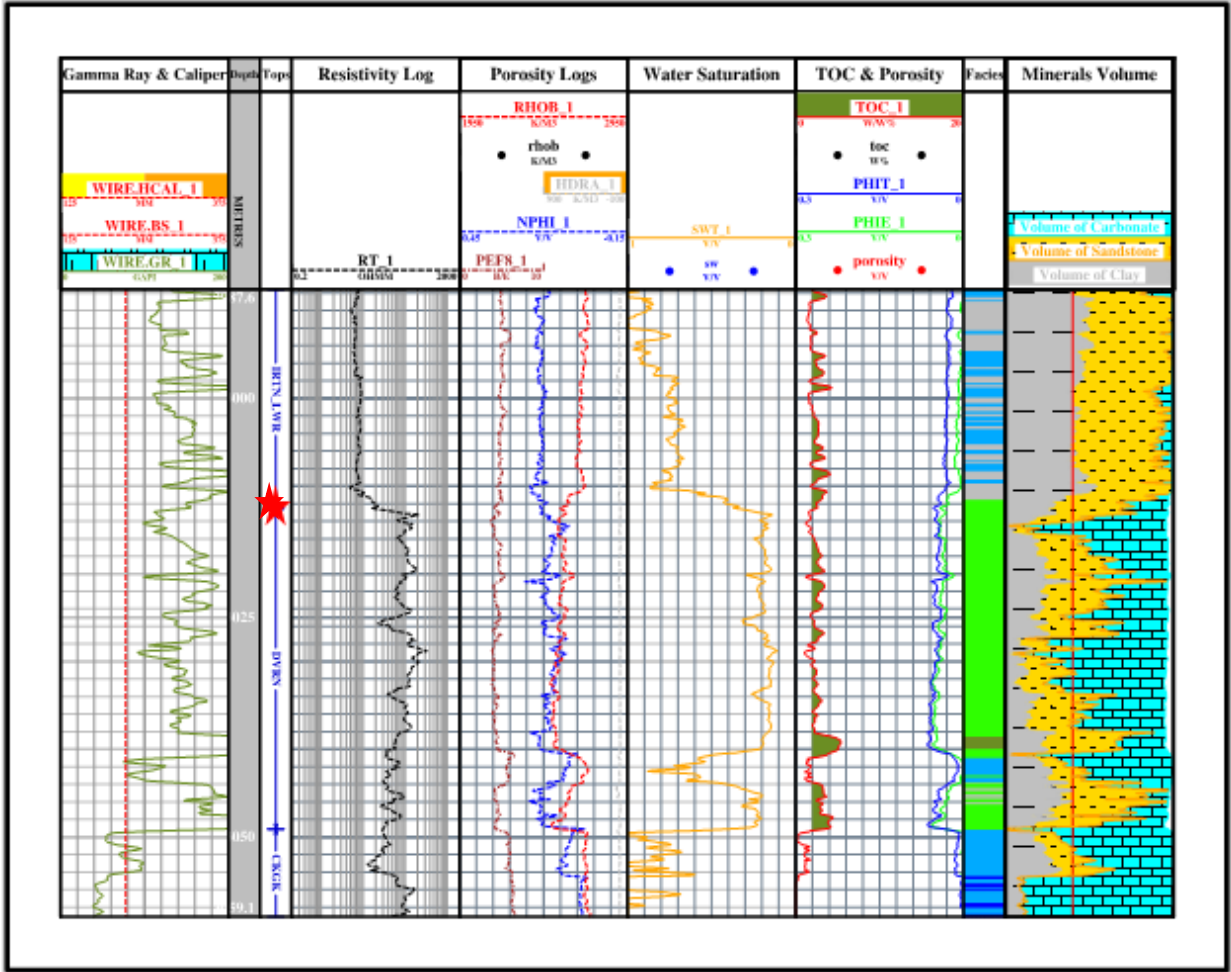


Figure 2.5.3 Well J plot

### Chapter 3: Petrophysical facies building

The facies distribution and definition is based on Multi-cluster analysis in Geolog to create electron facies. A comparison of facies and meaningful log derived parameters were done to subdivide or group similar facies, which represent the favorable zones.

The method that has been used is called MRGC – Multi-Resolution Graph-Based Clustering.

MRGC is “A multi-dimensional dot-pattern recognition method based on non-parametric k-nearest neighbors and graph data representation. The underlying structure of the data is analyzed and natural data groups are formed that may have very different densities, sizes, shapes, and relative separations. MRGC automatically determines the optimal number of clusters, yet allows the geologist to control the level of detail actually needed to define the electrofacies.” (Geolog® 7.1 – Paradigm™ 2011.3)

#### 3.1 MRGC facies

For an unconventional reservoir evaluation, the target zone BVH (hydrocarbon volume, calculated from  $\text{Phit}^*(1-\text{Sw}_t)$ ), total organic carbon (TOC), and clay volume ( $V_{\text{clay}}$ , or called  $\text{vol\_illite}$  in some screen captures) are three key components to describe the unconventional reservoir qualities, which are parameters that have been derived from petrophysical modelling.

The three parameters (all from Log calculation) distributions are in Figure 3.1.1. The BVH, bulk volume hydrocarbon, derived from  $\text{Phit} * (1-\text{Sw}_t)$ , has a range from 0-0.1 v/v. The histogram of BVH shows two separated distributions. The first one is about lower than 0.015 v/v, with a peak close to zero, which describes the non reservoir situation.

Another trend is between 0.08- 0.015v/v, with a Gaussian like distribution, and peak around 0.05v/v.

TOC has a big trunk below 2%, which is considered non unconventional reservoir. The high TOC could reach 9%, but the mean is only 2.5%.

The Clay volume (vol\_Illite in the Figure 3.1.1) has two peaks, and the volume between 30 – 60% is reflective of non-reservoir.

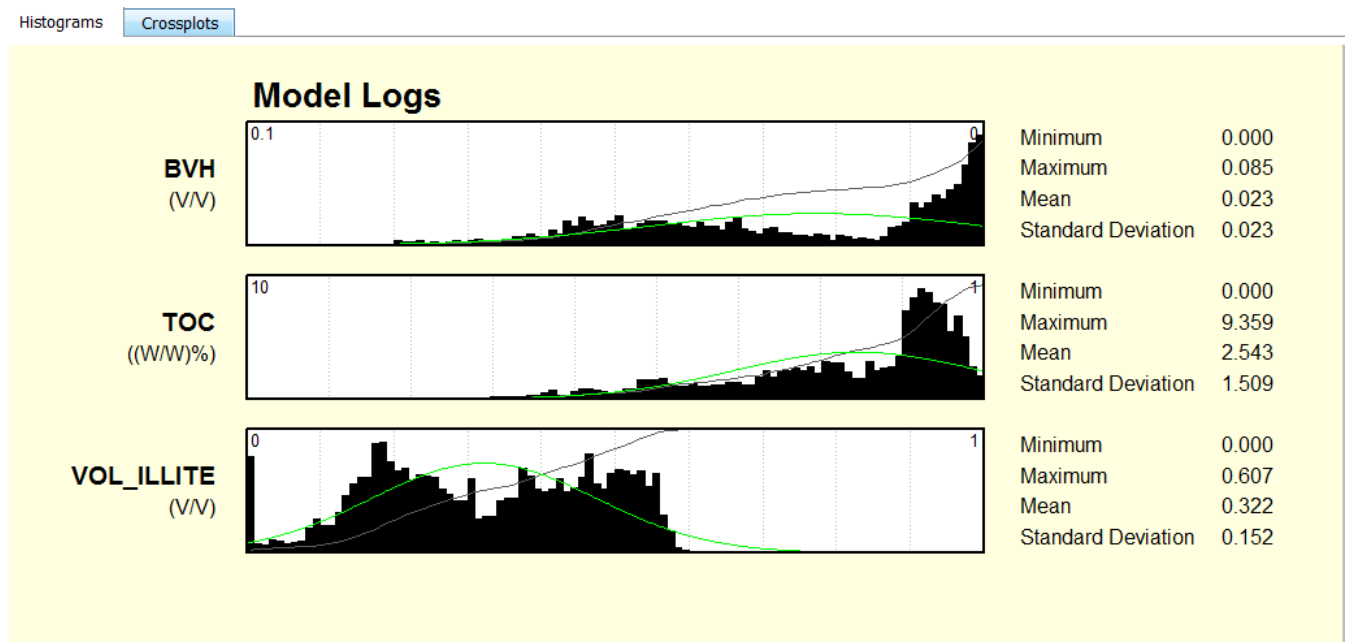


Figure 3.1.1 Three main petrophysical import distributions histogram

### 3.2 Model building

The eight cored wells have been used to define facies, because the petrophysical log properties are confirmed with core analyzed results, these can be used to describe/or separate the different facies.

Since the project is for exploration purposes and will be used in modeling software, the facies are not too complicated. The expected output facies number is preset as

between 3-7. Though playing with cored wells, the Geolog MRGC auto run facies is hard to be lower than 5. Therefore, the initial minimum of Electrofacies has been set as 5, and the maximum is set to 25. The number of optimal models is 5, though it could go up to 25. The initial Neurons are set as 4, as Figure 3.2.1.

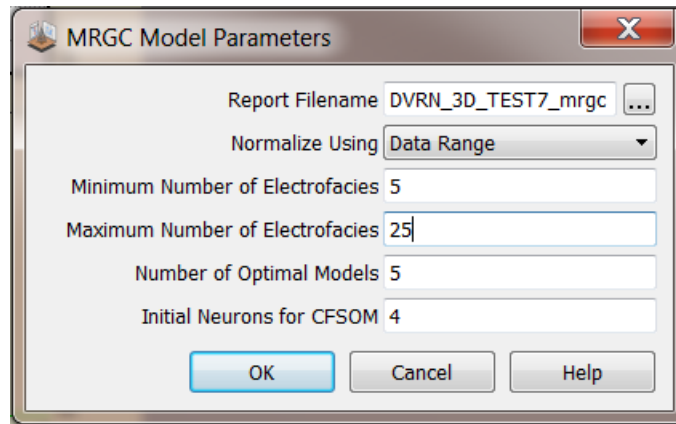


Figure 3.2.1 MRGC Model Parameters

After auto computing, there are three output clusters, MRGC\_7\_CLUST, MRGC\_10\_CLUST, and MRGC\_12\_CLUST. The minimum auto facies (7 clusters) are shown with the three inputs distributions as Table 3.2.1 and Figure 3.2.2.

Table 3.2.1 MRGC\_7\_CLUST mean values for different facies

FACIES	WEIGHT	BVH	TOC	VOL_ILLITE
1	6	0.01	1.13	0.20
2	1046	0.06	5.47	0.18
3	2772	0.04	3.32	0.21
4	362	0.03	2.64	0.36
5	3321	0.01	1.69	0.49
6	1469	0.00	1.43	0.32
7	305	0.00	0.00	0.01

Facies 1 (black) has too low weight (6), so it is not considered representative. The BVH (bulk volume of hydrocarbon) is 0.01v/v, and TOC is 1.13 w%; plus intermedia to clay (vol\_illite, 0.2 v/v); therefore, facies 1 is considered non reservoir.

Facies 2 (dark green) is the dominant facies in this study, which has the highest BVH (0.06v/v), TOC (5.47w %), and relative low clay volume (0.18 v/v).

Facies 3 (light green) is the second best facies, with BVH 0.04 v/v, TOC 3.32w%, and 0.21v/v clay volume.

Based on the data distribution, facies 2 and 3 are considered reservoir facies; Comparing the facies 2 (dark green) and 3(light green) in the Figure 3.2.3, the facies 2 has much higher BVH and TOC; though there is some overlap in distributions. The clay volume is very similar.

Facies 4 (orange) and 5 (grey) have much higher clay volume (0.36v/v, 0.45v/v), compared to the previous facies, and have medium to low BVH (0.03v/v, 0.01v/v), and TOC (2.64w %, 1.69w %).

Facies 6(cyan) and 7(dark blue), BVHs are close to 0 v/v, which are considered to be non-reservoir, and the TOCs are 1.43, and 0, which are considered not effective hydrocarbon generation zones. Clay volumes are 0.32v/v, and 0.01v/v. They all have low porosity.

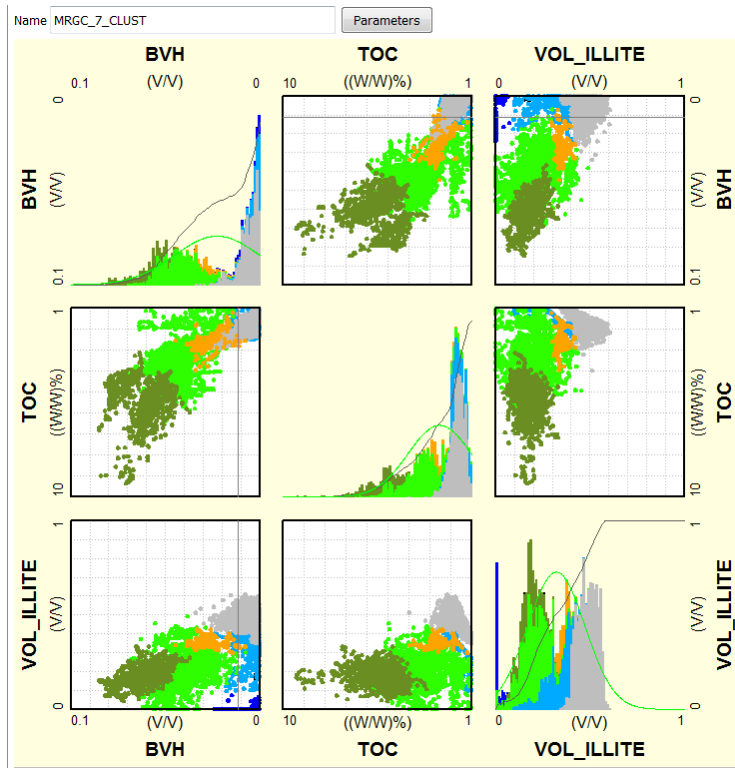


Figure 3.2.2 MRGC\_7\_CLUSTER three inputs crossplot

Due to the lack of representative data points in facies 1, it has been merged with facies 6 as “low porosity” facies, given the similar BVH and TOC reading.

Similarly, facies 4 and 5 have been put together with higher clay volume ( $> 0.35$  v/v), which is more ductile rock and a potential

frac barrier.

So, the final facies are:

1. Facies 6 and 1 (cyan), low porosity rock, none reservoir
2. Facies 2 (dark green), best rock and main target
3. Facies 3 (light green), secondary quality reservoir
4. Facies 4 and 5 (grey), none reservoir, high clay, as frac barrier

5. Facies 7 (dark blue), mainly carbonate (limestone), under the Duvernay formation

The detailed data distribution histogram is shown in Figure 3.2.3. BVH (bulk volume hydrocarbon) from left to right is from high to low; same as TOC distribution from left to right is from high to low; where as the clay volume Vol\_Illite distribution from left to right is from low to high.

The three data distribution trends represent reservoir quality from left to right as being from “good” to “bad”. Facies 2 and 3 have highest BVH, highest TOC, and relative low clay volume(vol\_Illite), indicating good reservoir quality.

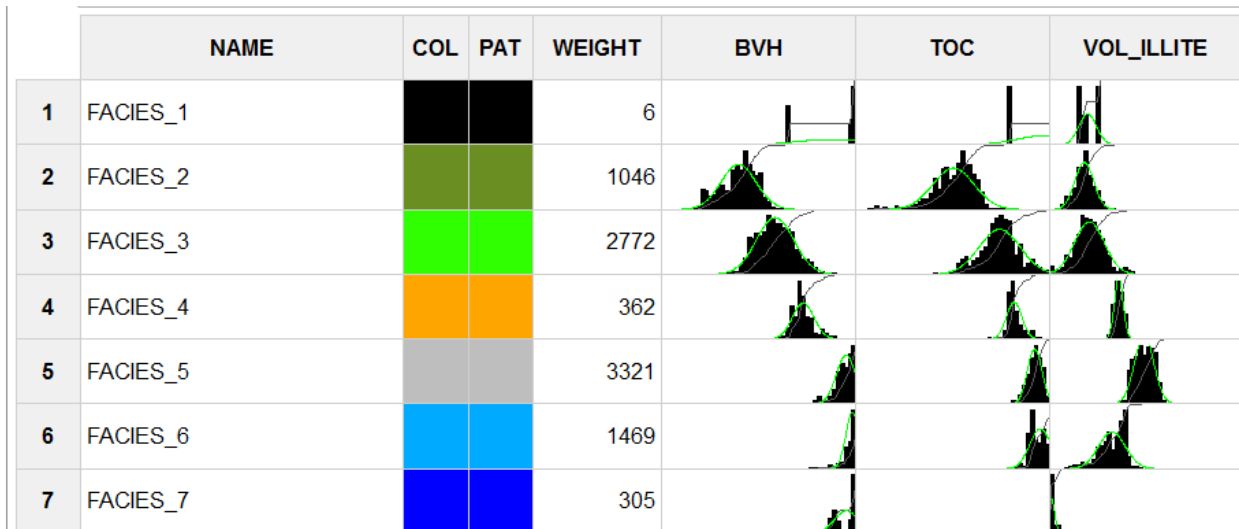


Figure 3.2.3 facies detail distribution

## Chapter 4: 3-D model building

The 3-D model was built using all petrophysical properties, and log derived facies using Petrel.

### 4.1 study area

The Petrel working region is limited by the reef boundaries in the southwest, and the focus area of the Duvernay target zone in the Kaybob area in the North East, as shown Figure 4.1.1. The color dots are the wells locations.

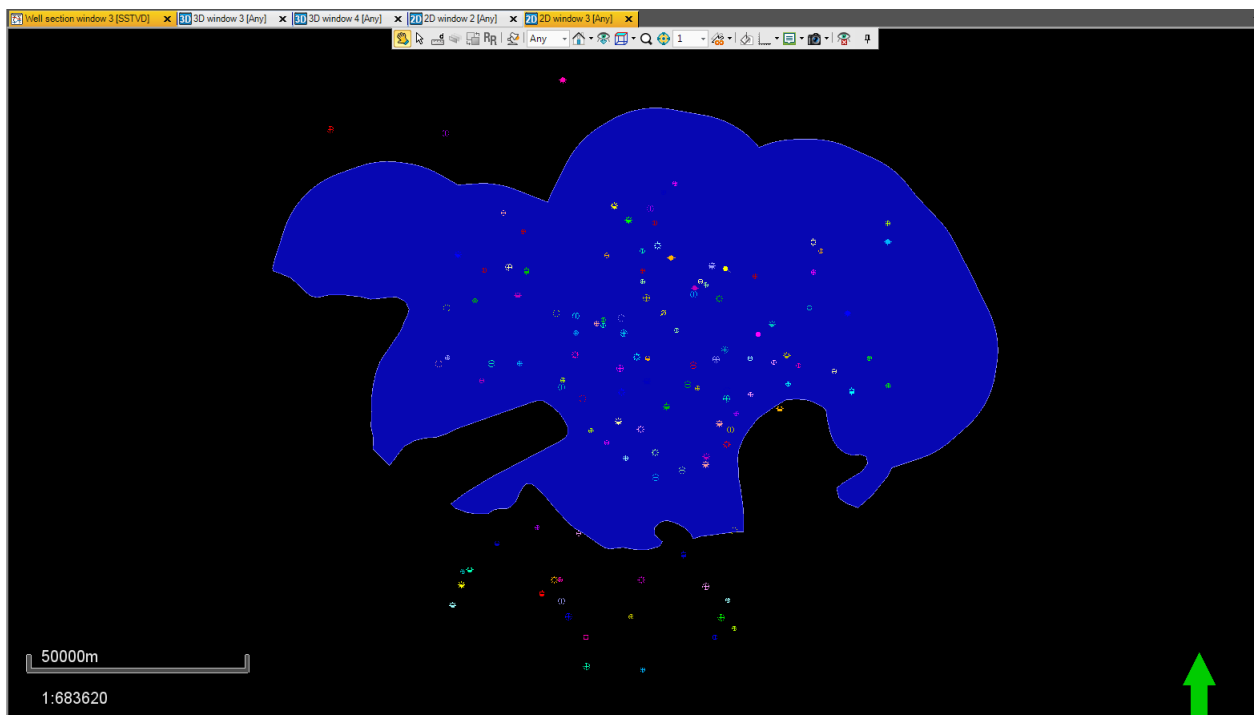


Figure 4.1.1 Duvernay working region and well location map

Figure 4.1.2 shows Duvernay formation is deepening in the southwest direction. The reservoir phases are changing North-East to South-West, from mainly oil to condensate, and then to gas.

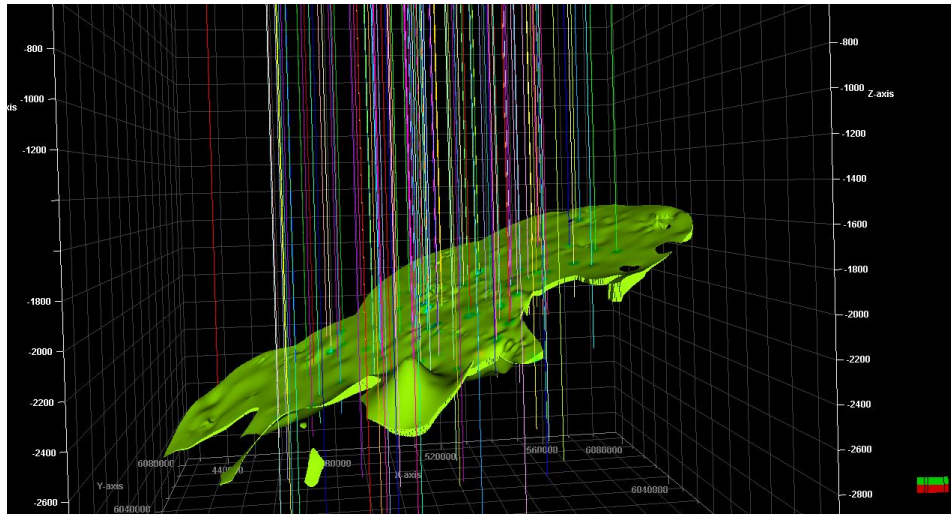


Figure 4.1.2 Duvernay formation in Petrel 3-D

In Petrel, all the petrophysical inputs, including Phit, Swt, Vclay, facies, and TOC are upscaled, then a kriging method is used to get the distribution plot in the Duvernay zone.

#### 4.2 Petrel 3-D output

Figure 4.2.1 shows BVH (bulk volume hydrocarbon) volume distribution plot. The color bar range is from 0 – 4%. The green area is the main target zone for Duvernay reservoir.

Figure 4.2.2 shows the clay volume average plot (color bar is from 0 -1, v/v), which shows the opposite in comparison to the BVH plot. The high BVH part shows low average clay volume, and vice versa. However, even in the highest clay area (blue), the average clay volume is mostly lower than 40%. From those two plots, the better zone is in the green cover area in BVH plot, and the purple area in the average vclay plot.

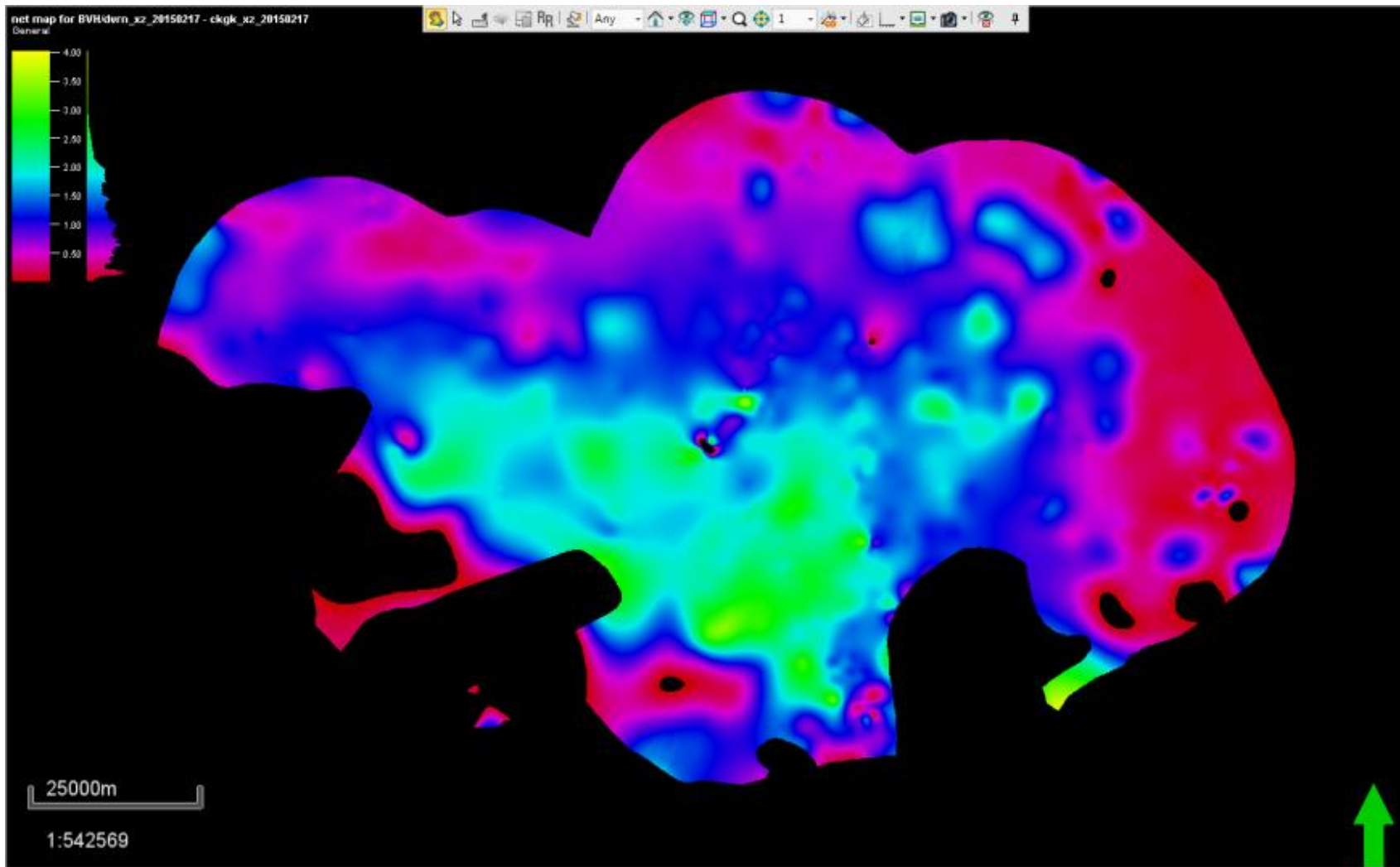


Figure 4.2.1 BVH net plot

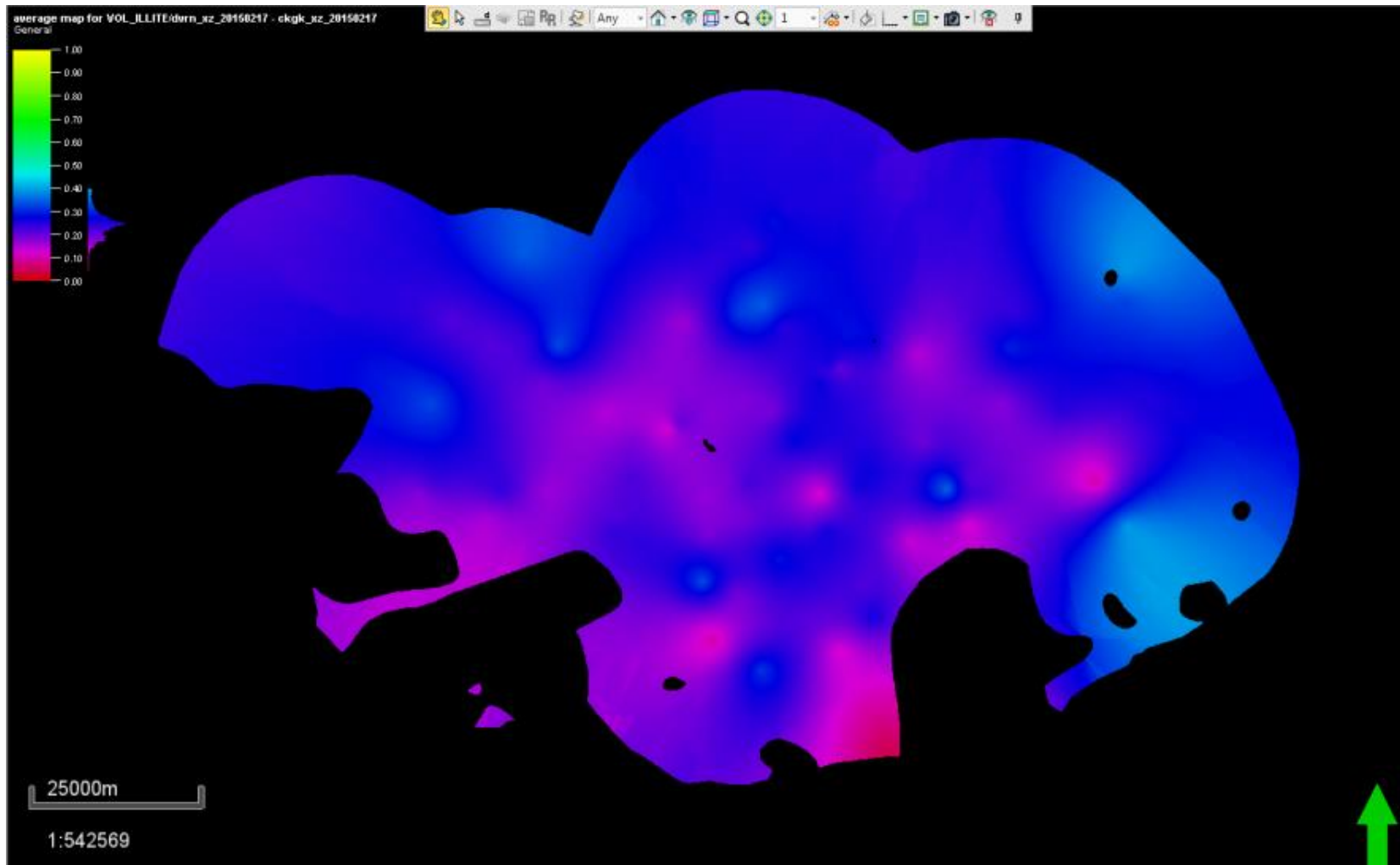


Figure 4.2.2 Average Clay plot

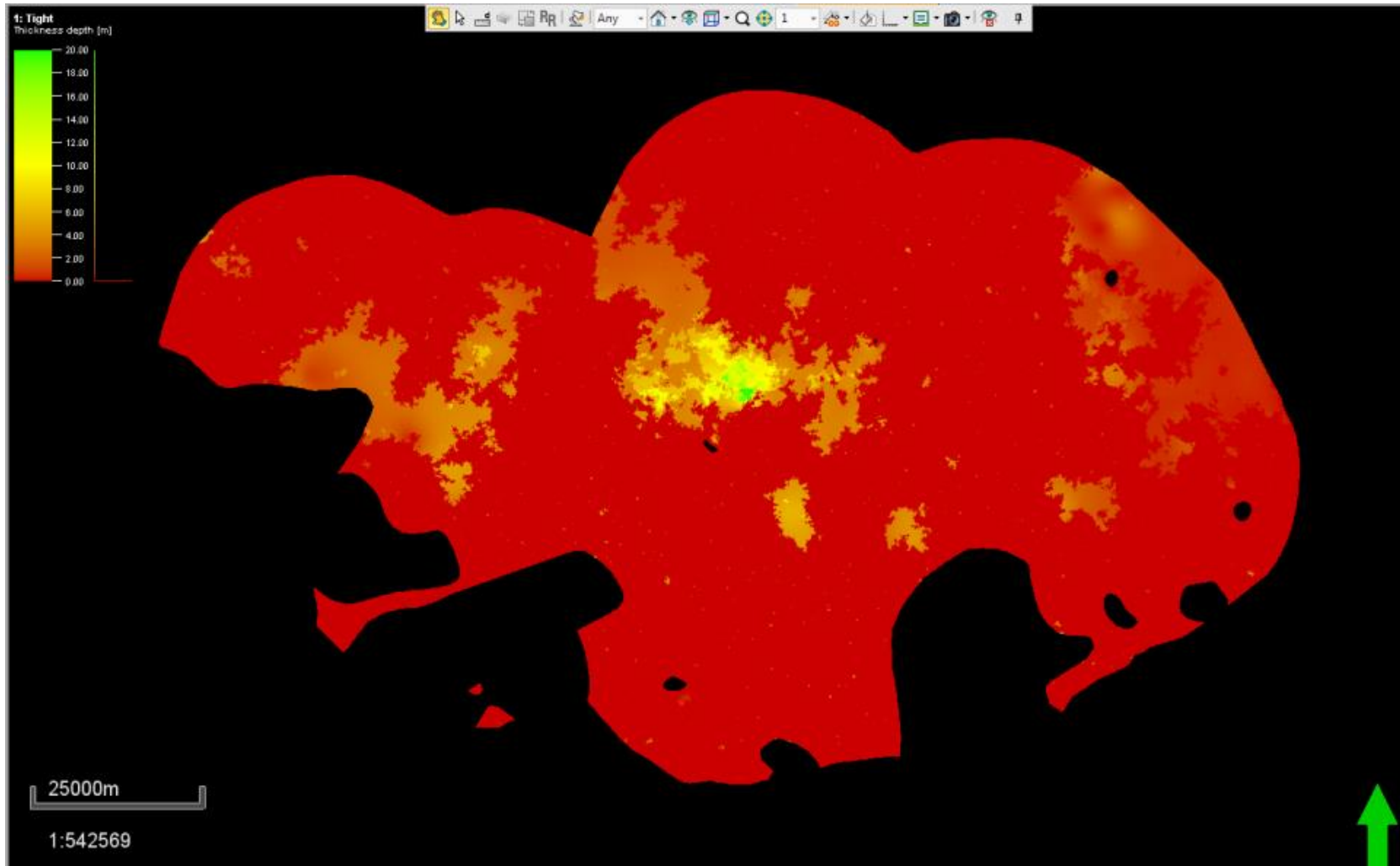


Figure 4.2.3 Low porosity facies 6 & 1 average thickness in Duvernay

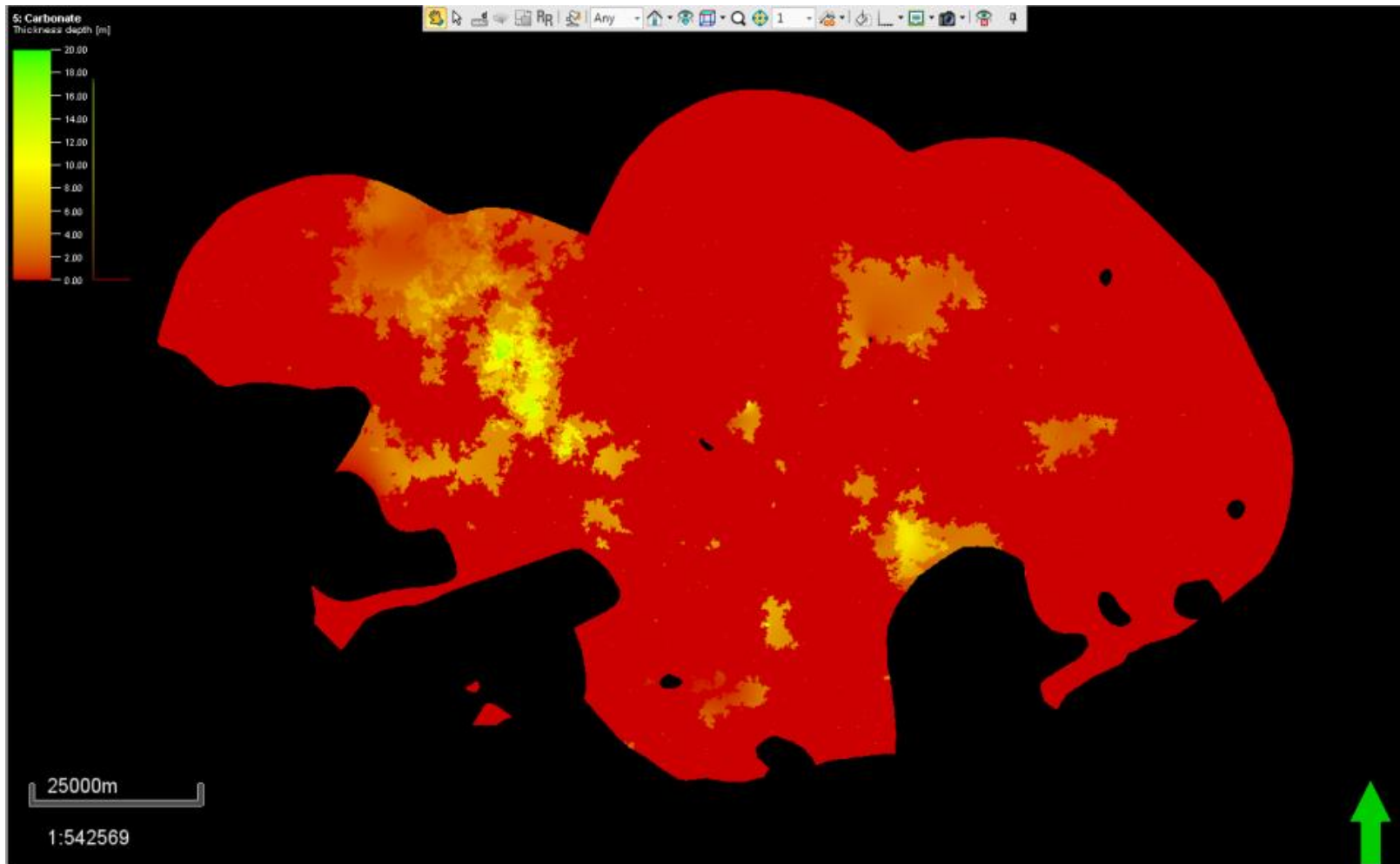


Figure 4.2.4 Carbonate facies average thickness in Duvernay

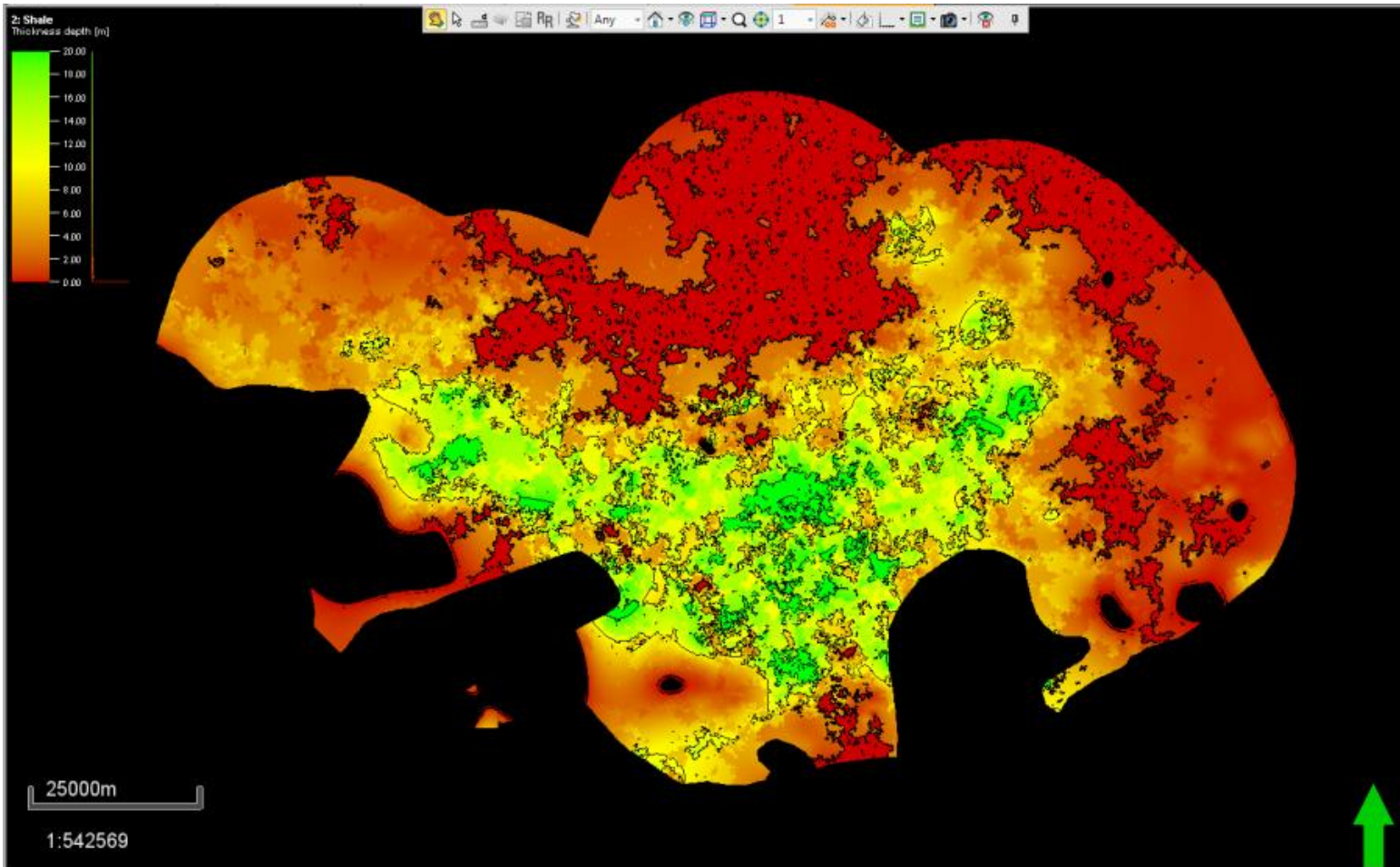


Figure 4.2.5 Facise 2 average thickness in Duvernay

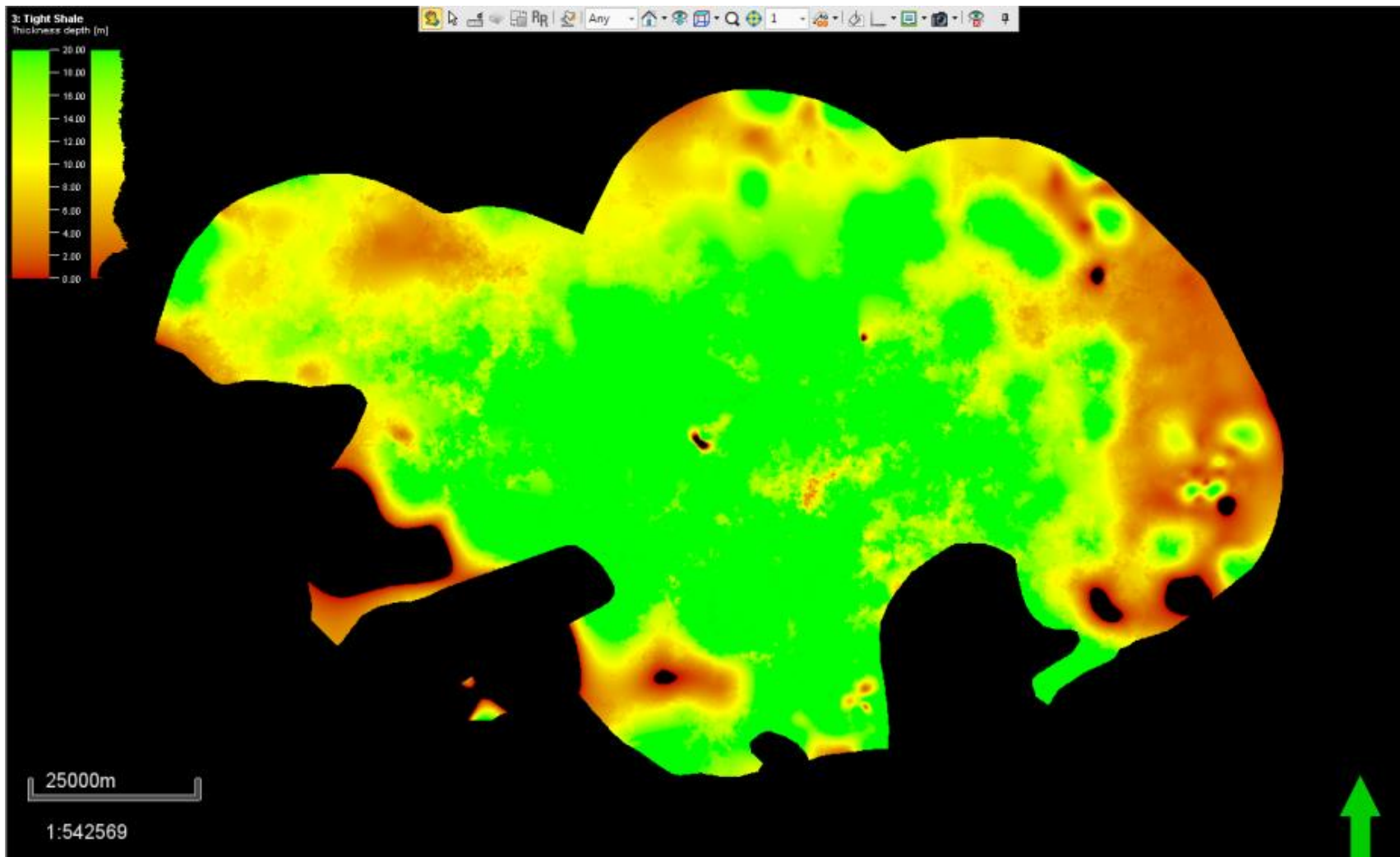


Figure 4.2.6 Facise 3 average thickness in Duvernay

Figure 4.2.3 and Figure 4.2.4 show “low porosity” and “Carbonate” facies average thickness in Duvernay Zone, which are relatively thin and not considered in the Duvernay zone. The color bar scales from 0 to 20 meters.

Figure 4.2.5 is the “best facies” thickness plot, and is considered to be the main target. The color bar is scaled from 0 to 20 meters. The thick area is located in the green area, this is similar with high BVH located area.; The green areas are thicker than 20 meters.

Figure 4.2.6 is the second best facies, and is also considered to be reservoir. This facies almost covers the entire Duvernay area. The color bar is scaled between 0 to 20 meters.

From BVH and Vclay average plots and facies thickness distribution plots, the petrophysically decent area is located in Figure 4.2.5 as the green area.

## Chapter 5: Comparison of the model result to production data

The Duvernay Kaybob area production data was collected from AccuMap software, based on three month accumulated liquid production.

### 5.1 Duvernay Kaybob area production distribution

Figure 5.1.1 shows average daily rates for the first 3 producing months. The size ranges from 2 m<sup>3</sup> fluid/day to the maximum outstanding well at 2,337 m<sup>3</sup> fluid/day.

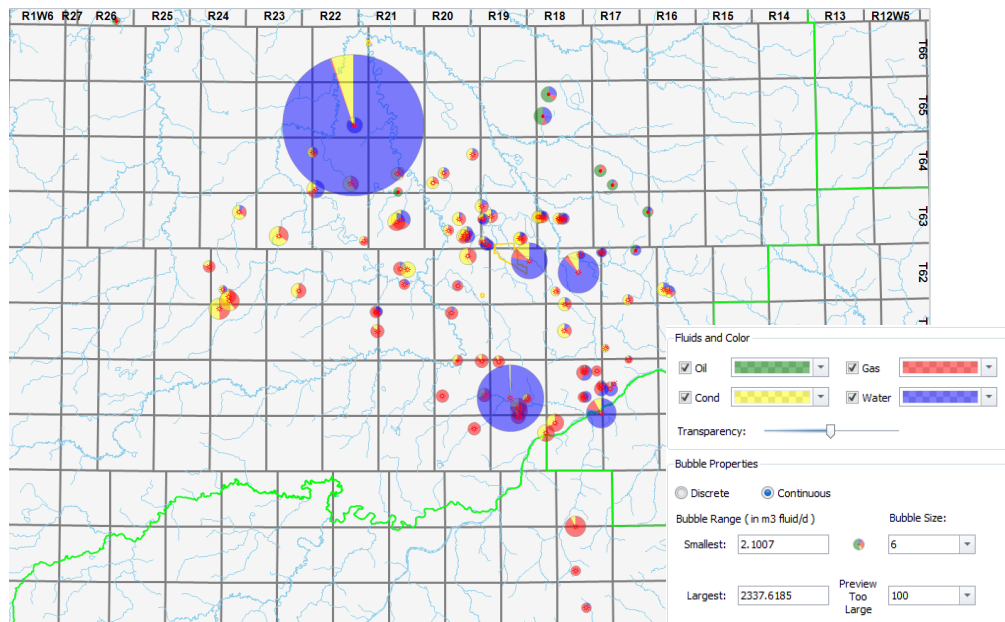


Figure 5.1.1 Duvernay Kaybob area liquid production rate (from AccuMap)

The average Duvernay Kaybob area water saturation average is very low, with no high water saturated area presented; therefore, the high production of water is assumed not to be from Duvernay zone.

Figure 5.1.2 shows production without high water production wells.

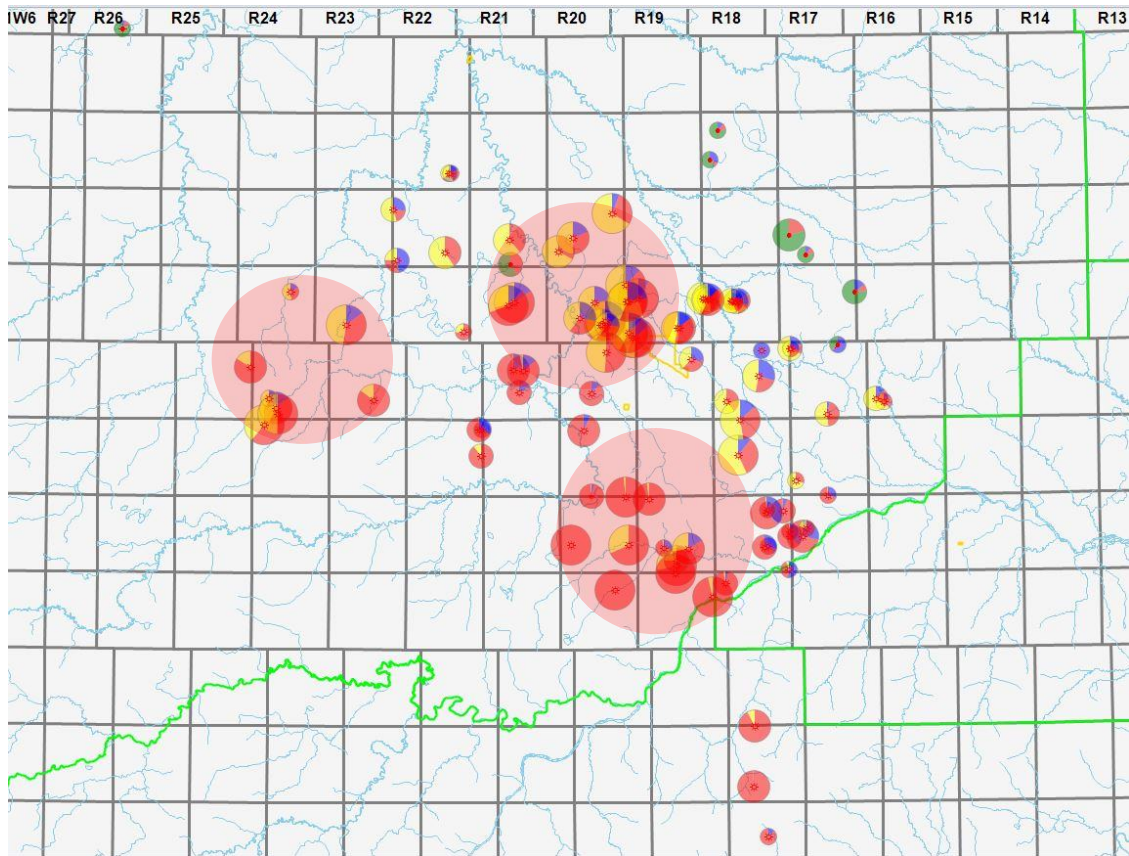


Figure 5.1.2 Duvernay Kaybob area liquid production rate (without high volume water)

From Figure 5.1.2, three high hydrocarbon producing zones are identified as: T61R20-T60R19, T63R24-T62R23, and T64R21-T63R20, as pink shaded areas.

## 5.2 Facies and production relationship

Since facies 2 and 3 are reservoir facies, the township based average thickness of facies 2 and 3 has been compared with single wells hydrocarbon production EOR (Table 5.2.1 and Figure 5.2.1.) There is no clear relationship between single well production and facies 2+3 thickness. In Figure 5.1.2, well 09-31-061-24W5, because it

has high production rate with low thickness, seems anomalous. It is high lighten in table 5.2.1.

o+c+g/6 vs. f23 avg thk

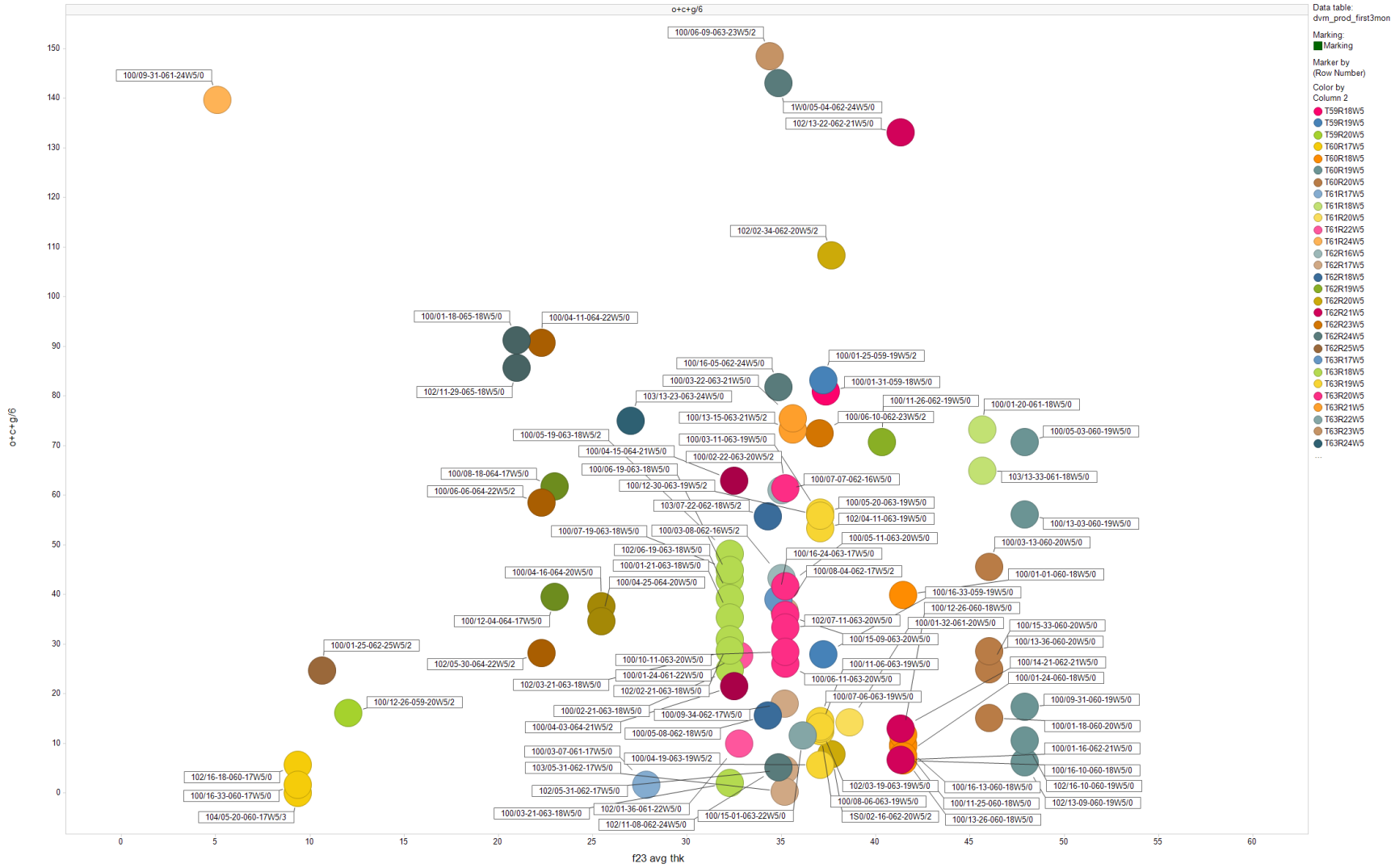


Figure 5.2.1 Duvernay Kaybob township based well production vs. facies thickness

Table 5.2.1 Duvernay Kaybob area first three month normalized hydrocarbon daily rate

<i>dvrn_prod_first3mon</i>					
		<b>Avg Dly Oil First(3) Prod (m3/d)</b>	<b>Avg Dly Gas First(3) Prod (E3m3/d)</b>	<b>Avg Dly Cond First(3) Prod (m3/d)</b>	<b>Equivalent Oil (m3/d)</b>
100/01-31-059-18W5/0	T59R18W5	0.0	128.2	59.5	80.9
100/01-25-059-19W5/2	T59R19W5	0.0	99.9	66.5	83.2
100/16-33-059-19W5/0	T59R19W5	0.0	105.4	10.4	28.0
100/12-26-059-20W5/2	T59R20W5	0.0	95.9	0.2	16.2
102/16-18-060-17W5/0	T60R17W5	0.0	13.5	3.4	5.6
104/05-20-060-17W5/3	T60R17W5				0.0
100/16-33-060-17W5/0	T60R17W5	0.0	4.9	0.9	1.7
100/01-01-060-18W5/0	T60R18W5	0.0	47.7	32.0	39.9
100/16-10-060-18W5/0	T60R18W5	0.1	38.5	0.0	6.5
100/16-13-060-18W5/0	T60R18W5	0.0	48.2	1.6	9.7
100/01-24-060-18W5/0	T60R18W5	0.0	37.4	1.2	7.4
100/11-25-060-18W5/0	T60R18W5	0.0	56.7	0.0	9.4
100/12-26-060-18W5/0	T60R18W5	0.0	59.8	1.8	11.8
100/13-26-060-18W5/0	T60R18W5	0.0	37.7	1.2	7.4
100/05-03-060-19W5/0	T60R19W5	0.0	121.4	50.5	70.8
100/13-03-060-19W5/0	T60R19W5	0.0	116.4	36.8	56.2
102/13-09-060-19W5/0	T60R19W5	0.0	0.0	6.1	6.1
102/16-10-060-19W5/0	T60R19W5	0.0	18.4	7.5	10.5
100/09-31-060-19W5/0	T60R19W5	0.0	69.2	5.9	17.4
100/03-13-060-20W5/0	T60R20W5	0.0	78.6	32.5	45.6
100/01-18-060-20W5/0	T60R20W5	0.0	89.9	0.2	15.1
100/15-33-060-20W5/0	T60R20W5	0.0	40.2	18.3	25.0
100/13-36-060-20W5/0	T60R20W5	0.0	100.2	11.9	28.6
100/03-07-061-17W5/0	T61R17W5	0.0	0.7	1.5	1.6
100/01-20-061-18W5/0	T61R18W5	0.0	28.1	68.6	73.3
103/13-33-061-18W5/0	T61R18W5	0.0	31.6	59.7	64.9
100/01-32-061-20W5/0	T61R20W5	0.0	85.4	0.0	14.2
100/01-24-061-22W5/0	T61R22W5	0.0	93.4	12.1	27.7
102/01-36-061-22W5/0	T61R22W5	0.0	55.9	0.6	9.9
100/09-31-061-24W5/0	T61R24W5	0.0	126.5	118.5	139.6
100/07-07-062-16W5/0	T62R16W5	0.0	24.0	57.0	61.0
100/03-08-062-16W5/2	T62R16W5	0.0	14.8	40.8	43.3
100/08-04-062-17W5/2	T62R17W5	0.0	21.8	33.0	36.6
102/05-31-062-17W5/0	T62R17W5	0.0	0.9	4.5	4.6
103/05-31-062-17W5/0	T62R17W5	0.0	0.5	0.1	0.2
100/09-34-062-17W5/0	T62R17W5	17.8	1.6	0.0	18.0
100/05-08-062-18W5/0	T62R18W5	0.0	9.9	13.9	15.6
103/07-22-062-18W5/2	T62R18W5	0.0	23.4	51.9	55.8
100/11-26-062-19W5/0	T62R19W5	0.0	49.6	62.5	70.7

1S0/02-16-062-20W5/2	T62R20W5	0.0	46.8	0.0	7.8
102/02-34-062-20W5/2	T62R20W5	0.0	72.8	96.3	108.4
100/01-16-062-21W5/0	T62R21W5	0.0	39.9	0.0	6.7
100/14-21-062-21W5/0	T62R21W5	0.0	77.2	0.1	12.9
102/13-22-062-21W5/0	T62R21W5	0.0	0.0	133.1	133.1
100/06-10-062-23W5/2	T62R23W5	0.0	76.7	59.7	72.5
1W0/05-04-062-24W5/0	T62R24W5	0.0	94.4	127.3	143.1
100/16-05-062-24W5/0	T62R24W5	0.0	64.2	71.1	81.8
102/11-08-062-24W5/0	T62R24W5	0.0	1.1	5.0	5.2
100/01-25-062-25W5/2	T62R25W5	0.0	61.2	14.5	24.7
100/16-24-063-17W5/0	T63R17W5	38.2	4.7	0.0	39.0
100/05-19-063-18W5/2	T63R18W5	0.0	29.5	43.3	48.2
100/06-19-063-18W5/0	T63R18W5	0.0	25.1	38.9	43.1
102/06-19-063-18W5/0	T63R18W5	0.0	21.0	35.8	39.3
100/07-19-063-18W5/0	T63R18W5	0.0	19.9	41.6	44.9
100/01-21-063-18W5/0	T63R18W5	0.0	11.6	33.4	35.4
100/02-21-063-18W5/0	T63R18W5	0.0	8.3	23.4	24.8
102/02-21-063-18W5/0	T63R18W5	0.0	10.7	29.2	31.0
100/03-21-063-18W5/0	T63R18W5	0.0	2.8	1.5	2.0
102/03-21-063-18W5/0	T63R18W5	0.0	12.1	26.6	28.6
100/07-06-063-19W5/0	T63R19W5	0.0	7.4	13.3	14.5
100/08-06-063-19W5/0	T63R19W5	0.0	5.8	11.5	12.4
100/11-06-063-19W5/0	T63R19W5	0.0	9.5	11.4	12.9
100/03-11-063-19W5/0	T63R19W5	0.0	33.1	50.3	55.8
102/04-11-063-19W5/0	T63R19W5	0.0	28.9	48.5	53.3
102/03-19-063-19W5/0	T63R19W5	0.0	6.4	12.3	13.4
100/04-19-063-19W5/2	T63R19W5	0.0	5.6	4.7	5.6
100/05-20-063-19W5/0	T63R19W5	0.0	37.9	50.2	56.5
100/12-30-063-19W5/2	T63R19W5	0.0	38.0	49.6	55.9
100/15-09-063-20W5/0	T63R20W5	0.0	25.2	31.6	35.8
100/05-11-063-20W5/0	T63R20W5	0.0	25.0	37.4	41.6
100/06-11-063-20W5/0	T63R20W5	0.0	16.0	23.4	26.0
102/07-11-063-20W5/0	T63R20W5	0.0	19.3	30.2	33.4
100/10-11-063-20W5/0	T63R20W5	0.0	18.5	25.4	28.5
100/02-22-063-20W5/2	T63R20W5	0.0	34.2	55.7	61.4
100/13-15-063-21W5/2	T63R21W5	0.0	81.4	59.7	73.3
100/03-22-063-21W5/0	T63R21W5	0.0	77.5	62.6	75.5
100/15-01-063-22W5/0	T63R22W5	0.0	22.9	7.7	11.5
100/06-09-063-23W5/2	T63R23W5	0.0	73.5	136.2	148.5
103/13-23-063-24W5/0	T63R24W5	0.0	29.9	70.0	75.0
100/12-04-064-17W5/0	T64R17W5	38.5	5.9	0.0	39.5
100/08-18-064-17W5/0	T64R17W5	58.8	17.9	0.0	61.8
100/04-16-064-20W5/0	T64R20W5	0.0	26.3	33.2	37.6
100/04-25-064-20W5/0	T64R20W5	0.0	32.3	29.3	34.6
100/04-03-064-21W5/2	T64R21W5	20.3	7.8	0.0	21.6
100/04-15-064-21W5/0	T64R21W5	0.0	34.1	57.2	62.9
100/06-06-064-22W5/2	T64R22W5	0.0	31.9	53.2	58.5

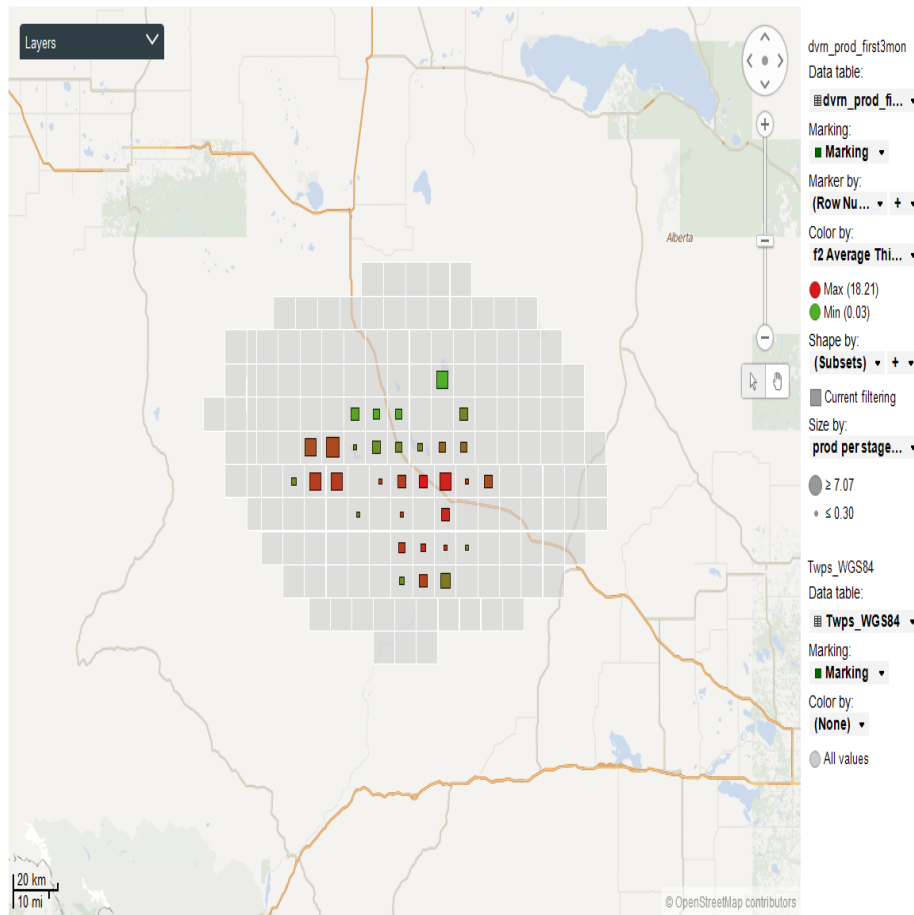
100/04-11-064-22W5/0	T64R22W5	0.0	58.3	81.0	90.7
102/05-30-064-22W5/2	T64R22W5	0.0	8.6	26.7	28.2
100/01-18-065-18W5/0	T65R18W5	88.5	16.6	0.0	91.2
102/11-29-065-18W5/0	T65R18W5	82.3	20.3	0.0	85.7

Equivalent oil = oil + condensate + gas/6

Next, the production wells were normalized by frac stage, and then averaged per township, to compare with facies average thickness per township, as Figure 5.2.2. The Figure 5.2.2a shows the township based normalized production. Color indicates the facies 2 thickness: red means thicker and green means thinner. The square size represents normalized production scale: the bigger square the higher normalized production.

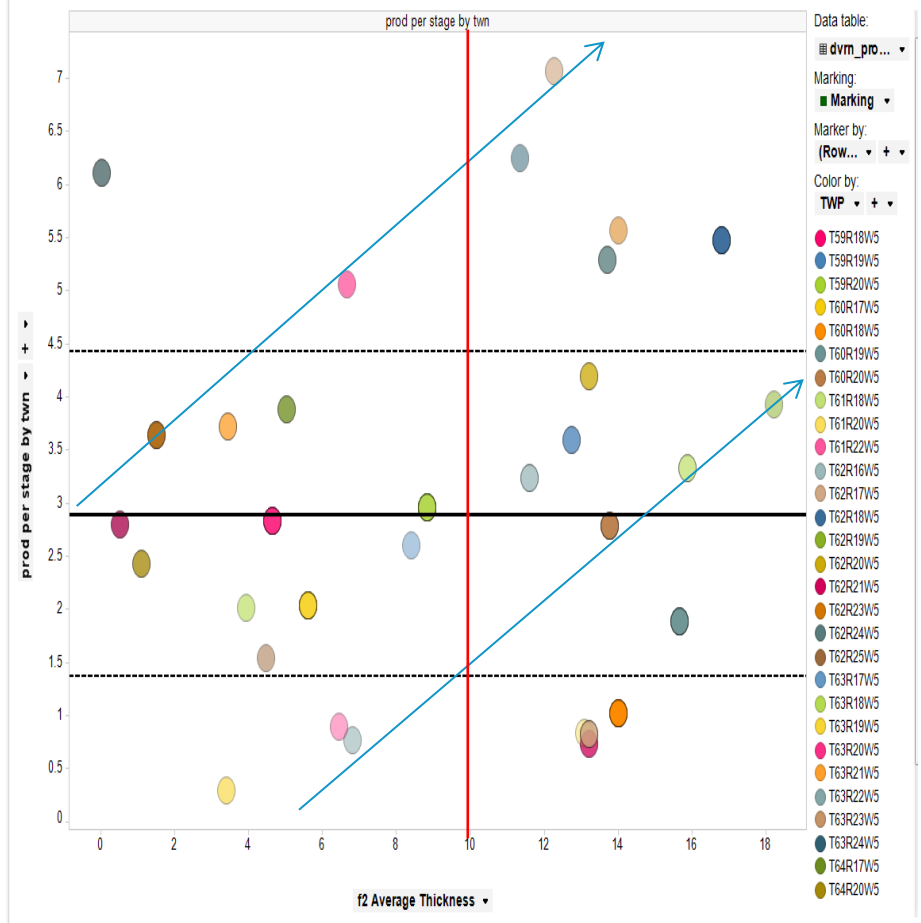
Figure 5.2.2b shows normalized production vs facies 2 thickness. There is a positive trend between the normalized production to facies 2 thicknesses, as shown with the blue lines.

### Map Chart



a. average thickness and production per township

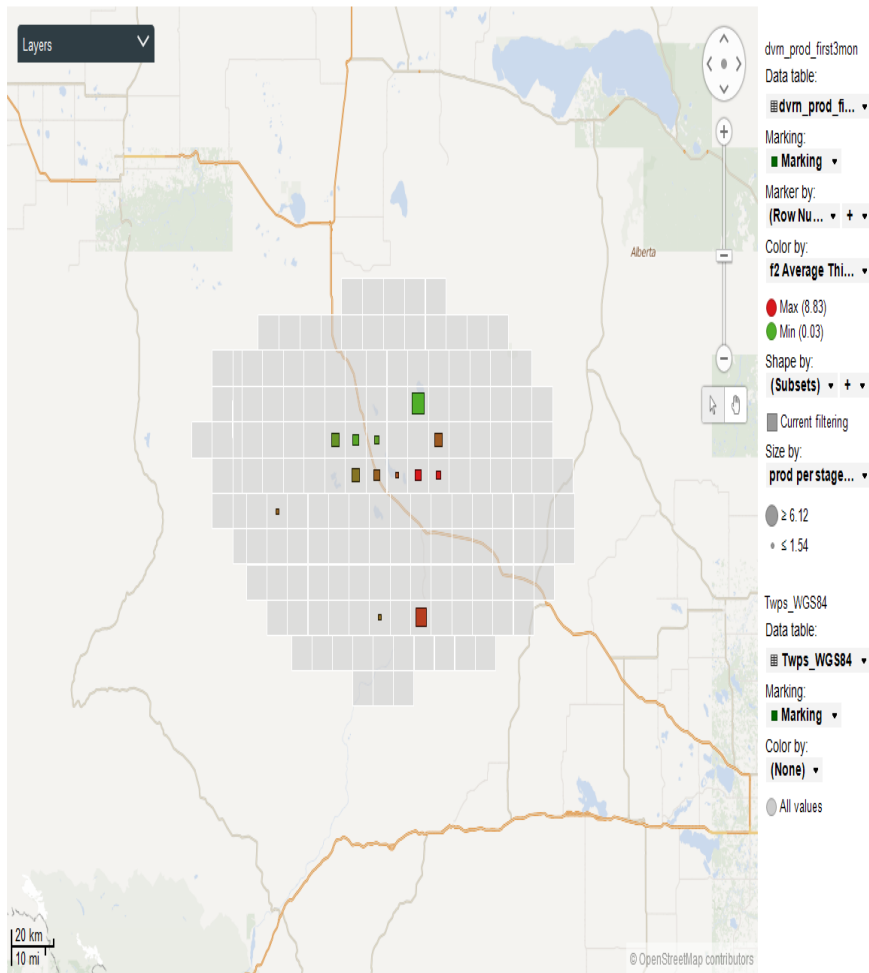
### prod per stage by twn vs. f2 Average Thickness



b. normalized production vs. facies 2 thickness crossplot

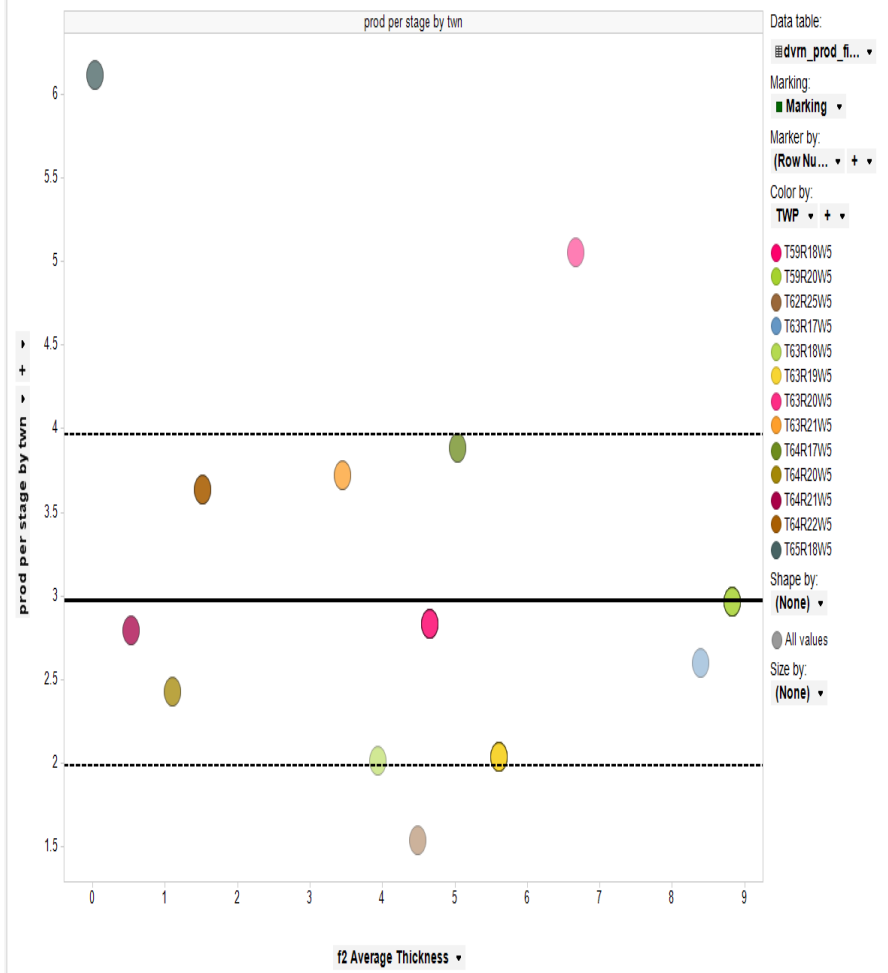
Figure 5.2.2 facies 2 thickness vs. production

### Map Chart



a. average thickness and production per township

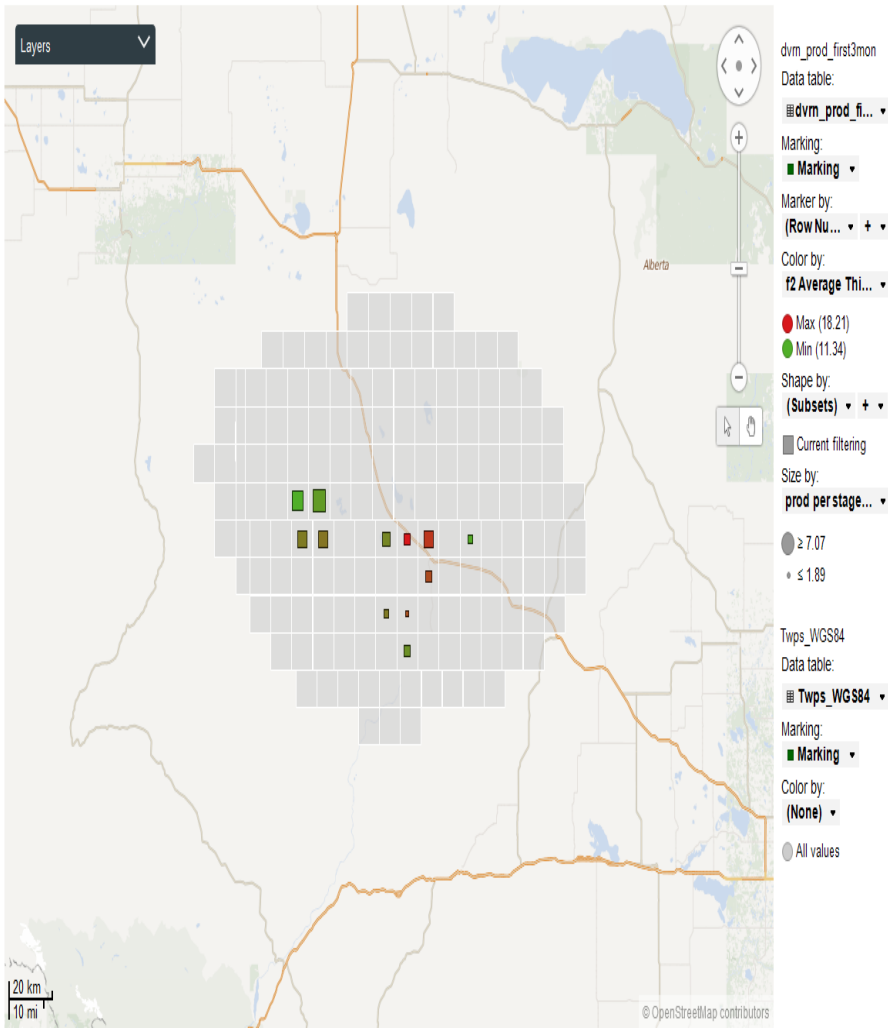
### prod per stage by twn vs. f2 Average Thickness



b. normalized production vs. facies 2 thinner wells crossplot

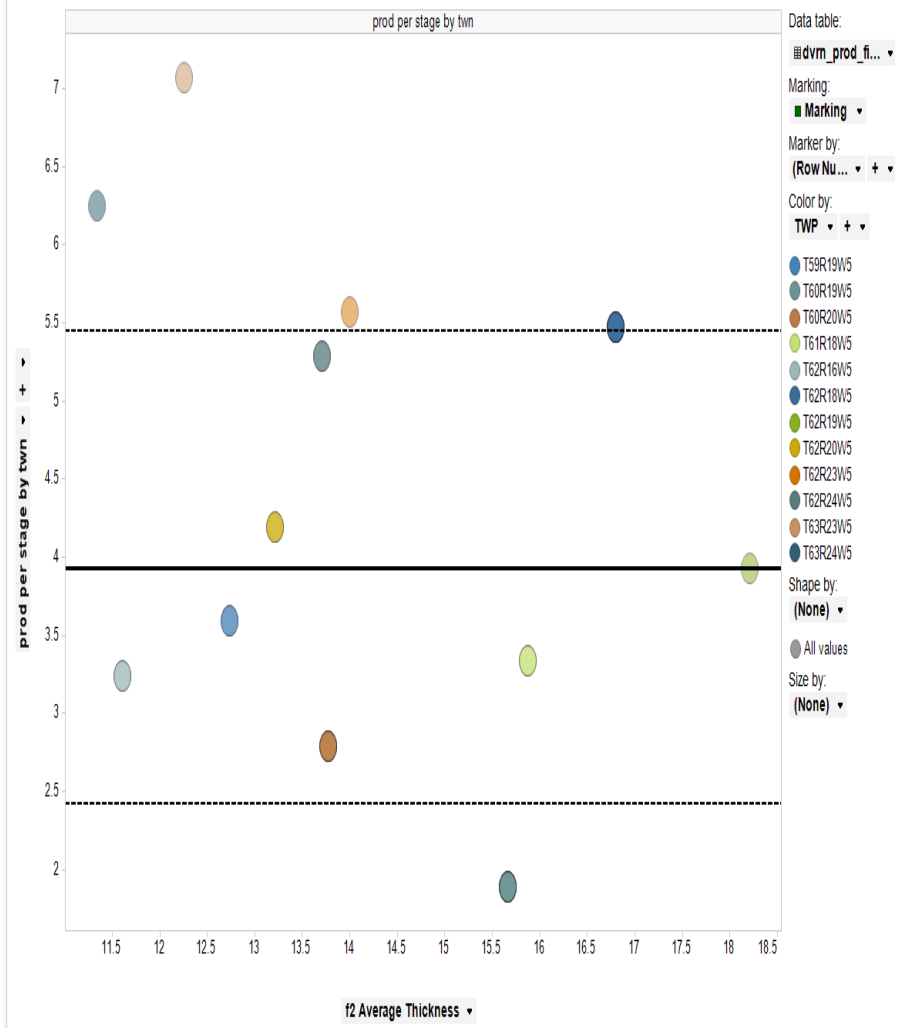
Figure 5.2.3 facies 2 thickness (< 10m) vs. production

### Map Chart



a. average thickness and production per township

### prod per stage by twn vs. f2 Average Thickness



b. normalized production vs. facies 2 thicker wells crossplot

Figure 5.2.4 facies 2 thickness (> 10m) vs. production

Visually checking the production data on Figure 5.2.2, it seems that two bins can be identified by splitting facies 2 thickness at a 10 meter cut off. When facies 2 thickness is below 10 meters, the production rates are relatively lower. As the wells approach the 10m thickness, the production rates are higher. The production data scatters more when the facies 2 thickness is greater than 10 meters.

Figure 5.2.3 and 5.2.4 show individual production averages, below and above 10 meters, removing values lower than 1.5 bbl/day/stage rate, which are considered non effective production numbers. In Figure 5.2.3, facies 2 is thinner than 10 meters, with an average of about 3 bbl/day/stage, and Figure 5.2.4 has an average of about 4 bbl/day/stage.

### 5.3 High grading area of greater than 10 meters in facies 2

As in Figure 5.3.1, the green area has a facies 2 thickness cut off of 10 meters, here there is the best potential from Petrophysical analysis, which should have a better chance to have good producing wells. The color bar scales from 0 to 20 meters, but anything thinner than 10 meters has been removed.

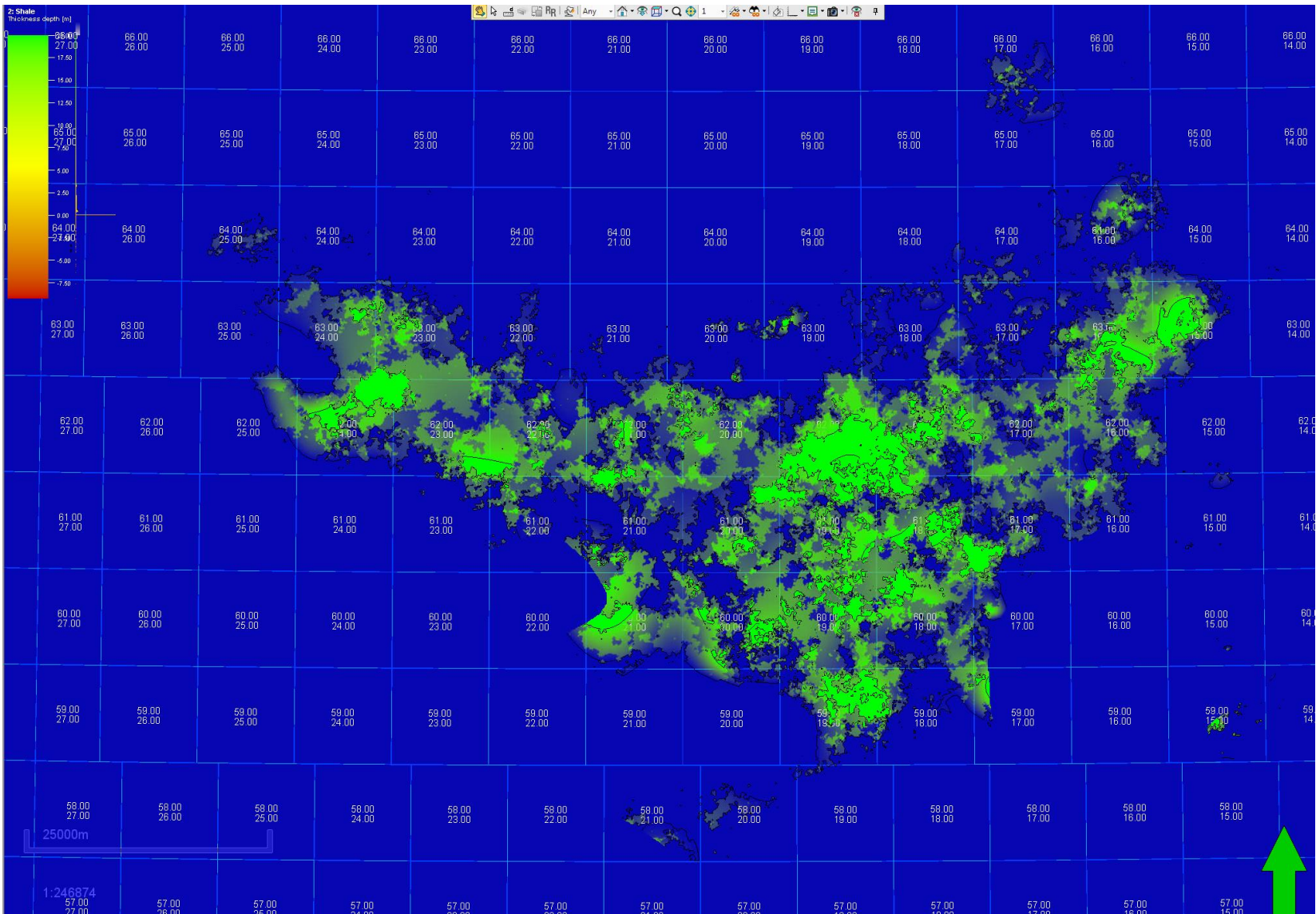


Figure 5.3.1 high lights future potential high production zones

## **Chapter 6: Experimental results and discussion**

Since the early stage production is the key for getting the investment payback, finding the best spots in the play is the most important task for unconventional exploration.

Through the study, the best facies and hydrocarbon volume can be used to get a high graded area; even though the comparison result shows there is no single answer to resolve all of the production problems. Petrophysical facies is one of the key components for finding high performance wells. Rock geomechanical properties, completion methodology, well pairs distance, stimulation strategy and production methodology all play very important roles in getting the best result.

Although petrophysical facies could not give the direct answer, I believe it provides the information necessary to target the best productive area.

## **Conclusions**

A petrophysical parameter-based and electron facies-controlled geological 3-D model gives a favorable unconventional play area and zone, which correlates positively with production results. Understanding the resource variability and uncertainty of the shale play will help to set up the development plan, and will assist in making the decision between land acquisition and joint venture investment.

## Bibliography

- Archie, G. E., 1942. The Electrical Resistivity Log as an Aid in Determining Some Reservoir Characteristics, *Petroleum Transactions of AIME* 146: 54–62.
- Bowman, T., 2010, Direct Method of Determining Organic Shale Potential from Porosity and Resistivity Logs to Identify Possible Resource Plays, AAPG, Search and Discovery Article #110128 (2010)
- Blakey, R.C., 1996, <http://jan.ucc.nau.edu/~rcb7/globaltext2.html>
- Dawson, F.M., 2012, Canadian Unconventional Resources Technical Innovation Creating Opportunities, CSUR
- Geolog® 7.1 – Paradigm™ 2011.3 With Epos 4.1 Data Management
- Low, W. S., 2012, Duvernay Shale, BMO capital Markets, <https://datarooms.ca.bmo.com/Login%20Page%20Document%20Library/ADLibrary/Presentations/BMO%20Duvernay%20DUG%20June%202012.pdf>
- Misko, R., 2014, Devonian Shales Regional Structural Setting, Nexen (internal study)
- Passey, Q.R., S. Creaney, J.B. Kulla, F.J. Moretti, and J.D. Stroud, 1990, A practical model for organic richness from porosity and resistivity logs: *AAPG Bulletin*, v. 74, p. 1777-1794.
- Pickett, G., R., 1973, Pattern recognition as a means of formation evaluation: *The Log Analyst*, vol. 14, no. 4, p. 3–11.
- Rokosh, C.D., Lyster, S., Anderson, S.D.A., Beaton, A.P., Berhane, H., Brazzoni, T., Chen, D., Cheng, Y., Mack, T., Pana, C., and Pawlowicz, J.G., 2012, Summary of Alberta's Shale- and Siltstone-Hosted Hydrocarbons, page 8
- Stastny, R. P., 2013, Delving into the Duvernay, Oilweek, 2013-Sep-17

Switzer et al, 1994, Alberta Geological Survey, Duvernay Fm Isopach and Lithofacies,

Fig 12.17 [p.177]